

# Thermal Development Test of the NEXT PM1 Ion Engine

John R. Anderson<sup>1</sup> and John Steven Snyder<sup>2</sup>

*Jet Propulsion Laboratory, California Institute of Technology, Pasadena, California, 91109*

John Van Noord<sup>3</sup> and George C. Soulas<sup>4</sup>

*NASA Glenn Research Center, Cleveland, Ohio, 44135*

NASA's Evolutionary Xenon Thruster (NEXT) is a next-generation high-power ion thruster under development by NASA, led by GRC and supported by JPL and Aerojet, as a part of the In-Space Propulsion Program. NEXT is designed for use on robotic exploration missions of the solar system using solar electric power. Potential mission destinations that could benefit from a NEXT Solar Electric Propulsion (SEP) system include inner planets, small bodies, and outer planets and their moons. This range of robotic exploration missions generally calls for ion propulsion systems with deep throttling capability and system input power ranging from 0.6 to 25 kW, as referenced to solar array output at 1 Astronomical Unit (AU). Thermal development testing of the NEXT prototype model 1 (PM1) was conducted at JPL to assist in developing and validating a thruster thermal model. NEXT PM1 performance prior to, during and subsequent to thermal testing are presented. Test results are compared to the predicted hot and cold environments expected missions and the functionality of the thruster for these missions is discussed.

## Nomenclature

$J_b$	=	beam current (A)
$J_d$	=	discharge current (A)
$J_{dcut}$	=	discharge cut back current (A)
$J_{dh}$	=	discharge cathode heater current (A)
$J_{nh}$	=	neutralizer cathode heater current (A)
$J_{nk}$	=	neutralizer keeper current (A)
$m_c$	=	cathode flow rate (sccm)
$m_m$	=	main flow rate (sccm)
$m_n$	=	neutralizer flow rate (sccm)
$V_a$	=	accelerator grid voltage (V)
$V_b$	=	beam voltage (V)

## I. Introduction

NASA's Evolutionary Xenon Thruster (NEXT)<sup>1-3</sup> is a next-generation high-power ion thruster under development by NASA. The NEXT program is led by GRC and supported by JPL, Aerojet and L-3 Communications Electron Technologies, Inc., with participation by Applied Physics Laboratory, University of Michigan and Colorado State University, as a part of the In-Space Propulsion Program. NEXT is designed for use on robotic exploration missions of the solar system using solar electric power. Potential mission destinations that could benefit from a NEXT Solar Electric Propulsion (SEP) system include inner planets, small bodies, and outer planets and their moons<sup>4-6</sup>. This range of robotic exploration missions generally calls for ion propulsion systems with deep throttling capability and system input power ranging from 0.6 to 25 kW, as referenced to solar array output at 1 Astronomical Unit (AU).

---

<sup>1</sup> Senior Engineer, Propulsion and Materials Engineering, 4800 Oak Grove Drive, MS 125-109, Member AIAA.

<sup>2</sup> Senior Engineer, Propulsion and Materials Engineering, 4800 Oak Grove Drive, MS 125-109, Member AIAA.

<sup>3</sup> Aerospace Engineer, Space Propulsion Branch, 21000 Brookpark Road/MS 16-1, Member AIAA.

<sup>4</sup> NEXT Co-Investigator, Space Propulsion Branch, 21000 Brookpark Road/MS 16-1, Senior Member AIAA.

As part of the development effort, environmental testing is being undertaken to verify that the thruster can survive launch and thermal loads expected during typical missions. This includes vibration testing and thermal vacuum testing. Prior to performing these tests a thermal development test (TDT) was performed on the NEXT prototype model (PM) thruster, PM1.

The NEXT thermal development test was conducted to aid in developing and validating a thermal model for the thruster. Data were recorded to document key thruster temperatures as a function of thruster operating conditions and thermal environment. Information obtained from this test was used to determine the reference temperature location and test conditions for the subsequent thermal vacuum test.

### **A. Test Objectives**

The NEXT thermal development test had two major objectives. One was to document key thruster temperatures as a function of thruster operating condition and thermal environments that would be encountered during a typical mission. The second was to validate the test support equipment, hardware, and procedures required to execute the planned subsequent thermal vacuum test (TVT).

The first objective required testing the thruster at selected points spanning the thruster throttle range at cold, ambient and hot conditions. Testing was required to determine if the cathode and/or the neutralizer heaters could be used to maintain thruster components within flight allowable limits under cold conditions. Testing was also required to ascertain thruster and thruster component temperature margins under worst case thermal loads identified from mission analysis. In addition testing to determine the external heat load required to first reach a thruster component temperature limit was desired.

The second objective included selection of the thruster reference temperature location. The thermal development test was also used to determine the appropriate test conditions for the TVT; this included cold soak temperatures and heat flux required for hot testing.

### **B. Temperature Limits**

Temperature limits for critical thruster components were specified for the magnets, propellant isolator, wire harnesses and also at the candidate temperature reference locations—thruster gimbal pads—used during the thermal development test. The do not exceed low temperature limit for the thruster was set at -230 C; however, to avoid xenon condensation in the feed system, the propellant lines and propellant isolators were required to be above -109 C during thruster starts. The do not exceed upper temperature limit was 360 C for the magnets, 265 C for the propellant isolators and was 260 C for the internal thruster wire harness. The external wire harness was originally limited to 150 C due to use of Tefzel jacketing; the limit was subsequently increased to 200 C to allow testing at the desired external heat loads.

### **C. Thruster Operating Points**

Testing of NEXT PM1 was conducted using laboratory power supplies. The thruster operating points used during the thermal development test are listed in Table 1. Nine operating conditions were run during the functional and thermal testing. The table lists the control settings for these operating points, as well as those for cathode ignition.

Seven parameters are controlled during normal thruster operation. The propellant flow rates to the discharge chamber ( $m_m$ ), cathode ( $m_c$ ), and neutralizer ( $m_n$ ) are controlled. Ion optics parameters—beam current ( $J_b$ ), beam voltage ( $V_b$ ), and accelerator grid voltage ( $V_a$ )—are set to maintain the fraction of propellant accelerated to high speed, to provide the desired kinetic energy to the beam ions, and to prevent electron backstreaming. The neutralizer keeper current ( $J_{nk}$ ) is set to maintain efficient neutralizer operation and to prevent the neutralizer from extinguishing during recycles.

Two other parameters are controlled during thruster starts. The discharge cathode ( $J_{dh}$ ) and neutralizer heater current ( $J_{nh}$ ) are maintained at the specified set point to heat the cathodes to thermionic emission temperatures. Once cathode or neutralizer ignition has occurred, the heater current to that component is turned off.

In addition to the control parameters two other parameters—discharge current ( $J_d$ ) and discharge cut back current ( $J_{dcut}$ )—are also listed in Table 1. During normal thruster operation, the discharge current is varied to provide the desired beam current. Nominal discharge currents are listed in the table to provide a reasonable set point during thruster starts prior to applying high voltage for beam extraction. The discharge current cut back is used during recycles, where the discharge current is cut back to a low value to avoid over current conditions while the high voltage is being ramped up. Because each of the thermal development test points has a unique combination of beam current  $J_b$  and beam voltage  $V_b$  these variables are used to identify the operating point throughout this report.

**Table 1. NEXT PM1 Throttle Table.**

Control Parameter	Ignition	Discharge Only	TDT 1	TDT 2	TDT 3	TDT 4	TDT 5	TDT 6	TDT 7	TDT 8
Jnh (A)	8.5	-	-	-	-	-	-	-	-	-
Jnk (A)	3.0	3.0	3.0	3.0	3.0	3.0	3.0	3.0	3.0	3.0
Jdh (A)	8.5	-	-	-	-	-	-	-	-	-
Jd (A)	9.0	9.0	8.0 <sup>a</sup>	9.5 <sup>a</sup>	8.8 <sup>a</sup>	8.4 <sup>a</sup>	14.7 <sup>a</sup>	13.9 <sup>a</sup>	20.6 <sup>a</sup>	18.9 <sup>a</sup>
Jdcut (A)	-	-	8.4	8.4	8.4	8.4	8.4	8.4	8.4	8.4
Jb (A)	-	-	1.00	1.20	1.20	1.20	2.00	2.00	3.52	3.52
Vb (V)	-	-	275	679	1179	1800	1179	1800	1179	1800
Va (V)	-	-	-500	-115	-200	-210	-200	-210	-200	-210
m <sub>m</sub> (sccm)	14.23	14.23	12.32	14.23	14.23	14.23	25.79	25.79	49.64	49.64
m <sub>c</sub> (sccm)	3.57	3.57	3.52	3.57	3.57	3.57	3.87	3.87	4.87	4.87
m <sub>n</sub> (sccm)	6.00	6.00	3.00	3.00	3.00	3.00	2.50	2.50	4.01	4.01

<sup>a</sup>Nominal Value; discharge current is adjusted to maintain a constant beam current.

## II. Test Hardware and Facilities

### A. Thruster

The NEXT PM1 is a 40 cm diameter prototype model thrusters fabricated by Aerojet<sup>7</sup> for GRC under the NEXT project. The thruster is capable of operation over a wide power envelope, from beam currents and voltages of 1.0 A, 275 V at the low end to 3.52 A and 1800 V at the high end of the throttle range.

The NEXT PM1 thruster used for the thermal development test was instrumented with 34 thermocouples. Twenty thermocouples were attached to high voltage components; seven were on magnet retainer rings, four were spot welded to the outside of the discharge chamber, three were on the ion optics, two were attached to the discharge cathode assembly, three were on wire harnesses and one was attached to a propellant isolator. Fourteen thermocouples were attached to low voltage surfaces; five were located at various locations on the plasma screen, three were mounted on the front mask, two were placed on the neutralizer assembly, one was on the neutralizer harness and one was spot welded to each of the three gimbal pads. These thermocouples were installed on PM1 prior to shipping to JPL. A list of the thermocouples used on PM1 during the thermal development test is provided in Table 2. The three columns in the table list the designation number, the component and the voltage for each of the NEXT PM1 thermocouples. In addition to the thruster thermocouples, thermocouples were also mounted on the gimbal flexures that interfaced between the PM1 gimbal pads and the thruster support structure during the thermal development test.

### B. Data Acquisition and Power Supply Control System

The thermal development test was performed using laboratory power supplies. These power supplies were controlled by data acquisition and control software. The data acquisition system uses Opto22 modules to read thruster currents, voltages, flow rates and temperatures; facility pressure and temperatures are also measured. The flow meters, voltage dividers and current shunts used to measure thruster data were calibrated prior to the thermal development test. The data acquisition software records thruster and facility data at a user specified rate. Typically data was recorded once a minute; however, during thruster starts or when thruster parameters were being varied the rate was often changed to once every ten seconds. The software used to record data was also used to control thruster power supplies and flow rates. The thruster operator could input the desired power supply and flow rate set points. Once the set points were entered the software made the appropriate adjustments to control the thruster operating parameters at the specified conditions.

### C. Thruster Test Facility

The thermal development test was conducted in the patio chamber facility at Jet Propulsion Laboratory. The vacuum chamber is 3 m diameter and 8.6 m long, and has 9 cryopumps. With the vacuum chamber configuration used for the thermal development test the effective pumping speed was as high as 160,000 l/s. To minimize facility backspitter rates the interior of the vacuum facility is lined with graphite panels. Diagnostic equipment—ExB probe and Faraday probes—were installed in the vacuum chamber.

**Table 2. Thermocouples on PM1.**

<b>HIGH VOLTAGE THRUSTER TC's</b>		
<b>TC #</b>	<b>Purpose</b>	<b>Potential</b>
H1	Front Magnet temperature (5 o'clock)	Anode
H1b	Front Magnet (1 o'clock)	Anode
H2	Cylindrical magnet temperature (3 o'clock)	Anode
H2b	Cylindrical Magnet (8 o'clock )	Anode
H3	Conical magnet temperature (3 o'clock)	Anode
H3b	Conical Magnet (8 o'clock)	Anode
H4	Cathode Magnet Temperature (3 o'clock)	Anode
H5	Measure discharge chamber temperature (7 o'clock) vs. stainless steel mesh temperature (7:30 o'clock) (8 o'clock)	Anode
H5b		Anode
H5c		Anode
H5d	On magnet shim exposed in cut-out (8:30 o'clock)	Anode
H6	Downstream harness temp. (11 o'clock)	Anode
H7	Propellant isolator temperature (2 o'clock)	Anode
H8	Cathode tube behind insulator (8 o'clock)	Cathode
H9	Measure temperature of sputter shield (3 o'clock)	Cathode
H10	Titanium stiffening ring (5 o'clock)	Cathode
H11	Screen grid support temperature (11 o'clock)	Cathode
H12	Accelerator grid support temperature (10 o'clock)	Accelerator
H13	Cathode harness support temperature (1 o'clock)	Anode (floating - packed in wire bundle)
H14	Upstream harness temp. (11 o'clock)	Anode
<b>GROUND/LOW VOLTAGE THRUSTER TC's</b>		
<b>TC #</b>	<b>Purpose</b>	
L1	Neutralizer Keeper Temperature (12 o'clock)	Neut Keep (Low Voltage)
L2	Neut. support temp.(moved to under Neut) (12 o'clock)	Ground
L3	Mask Temp. closest to optics (12 o'clock)	Ground
L3b	Middle mask temperature (6 o'clock)	Ground
L4	Mask Temp. closest to optics, (6 o'clock)	Ground
L5	Plasma screen / Mask interface (1 o'clock)	Ground
L5b	Plasma screen / Mask interface (6 o'clock)	Ground
L6	Spot weld to gimbal pad 1 (2 o'clock)	Ground
L6b	Spot weld to gimbal pads 2 (6 o'clock)	Ground
L6c	Spot weld to gimbal pads 3 (10 o'clock)	Ground
L8	Plasma screen cone / conical interface (1 o'clock)	Ground
L8b	Plasma screen cone / Conical interface (7 o'clock)	Ground
L9	Harness exit near Neutralizer (12 o'clock)	Ground
L10	Rear plasma screen temperature (3 o'clock)	Ground

Colors represent different potentials

NEXT PM1, shown in Figure 1, was installed in a 1.2 m diameter by 1.0 m long thermal shroud—provided by GRC—which was installed in the vacuum facility. The downstream end of the thermal shroud was located 6.2 m

from the downstream end of the vacuum facility. The thruster was mounted inside the shroud with the neutralizer keeper orifice plate located 5.7 cm from the downstream end of the shroud.

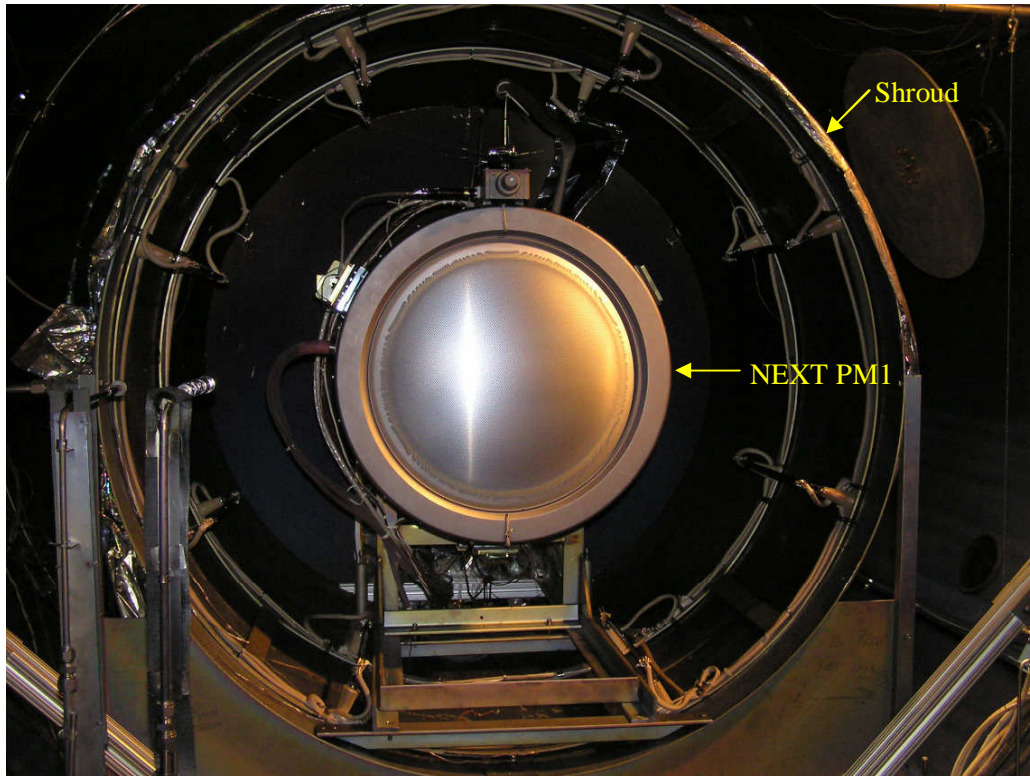


**Figure 1. NEXE PM1 Installed Inside Thermal Shroud.**

A schematic of the shroud thermocouple locations is shown in Figure 2 and the locations in the shroud are listed in Table 3. The first column in Table 3 lists the shroud thermocouple number. The second column lists the shroud surface to which the thermocouple is attached; most thermocouples were attached to the cylinder wall or the back wall, one was attached to the thruster support structure and one was attached to one of the copper tubes used for liquid nitrogen cooling. The third column lists the clocking which is the same as that for the thruster. Thruster clocking is with respect to viewing the upstream side of the thruster; the east wall of the shroud is toward the 9 o'clock position and west wall is toward the 3 o'clock position. The fourth column lists the distance from the open end of the shroud to the thermocouple for thermocouples mounted on the cylindrical wall or copper tube and distance from the shroud centerline for thermocouples mounted on the back wall.

The shroud could be cooled with liquid nitrogen and also had eight heat lamps installed inside it to provide external heat flux to the thruster. The 0.29 m long, 1 kW heat lamps were installed parallel to the thruster axis. The radial spacing between the lamps and the thruster was 0.24 m. The lamps were spaced 45 degrees apart azimuthally and aligned axially along the length of the thruster with one end of the lamp even with the front mask of PM1. The heat lamp controller was set up to vary the power to the lamps as required to maintain a control thermocouple at constant temperature set point.

In order to determine the heat flux to the thruster, heat flux coupons were developed for this test. The heat flux coupons consisted of painted aluminum sheet metal installed in a multi-layer insulation box with a 1x1 cm aperture to allow external radiation to impinge on the aluminum. Due to variations in the dimensions and uncertainties in the optical properties of the surfaces, the heat flux coupons were calibrated using a Kendall Mk IV radiometer<sup>8</sup> as a standard. Two heat flux coupons were used to monitor the thermal radiation to the thruster and a third coupon temperature was used to control the heat lamps. The top heat flux coupon was located 0.04 m above the neutralizer housing and 0.1 m behind the neutralizer keeper orifice plate. The bottom rear heat flux coupon was located 0.05 m below the thruster and 0.24 m behind the front mask. The bottom front heat flux coupon, used to control the heat lamps, was placed 0.05 m below the thruster and 0.12 m behind the front mask. The top heat flux sensor is shown in Figure 3 and the bottom heat flux sensors are shown in Figure 4.



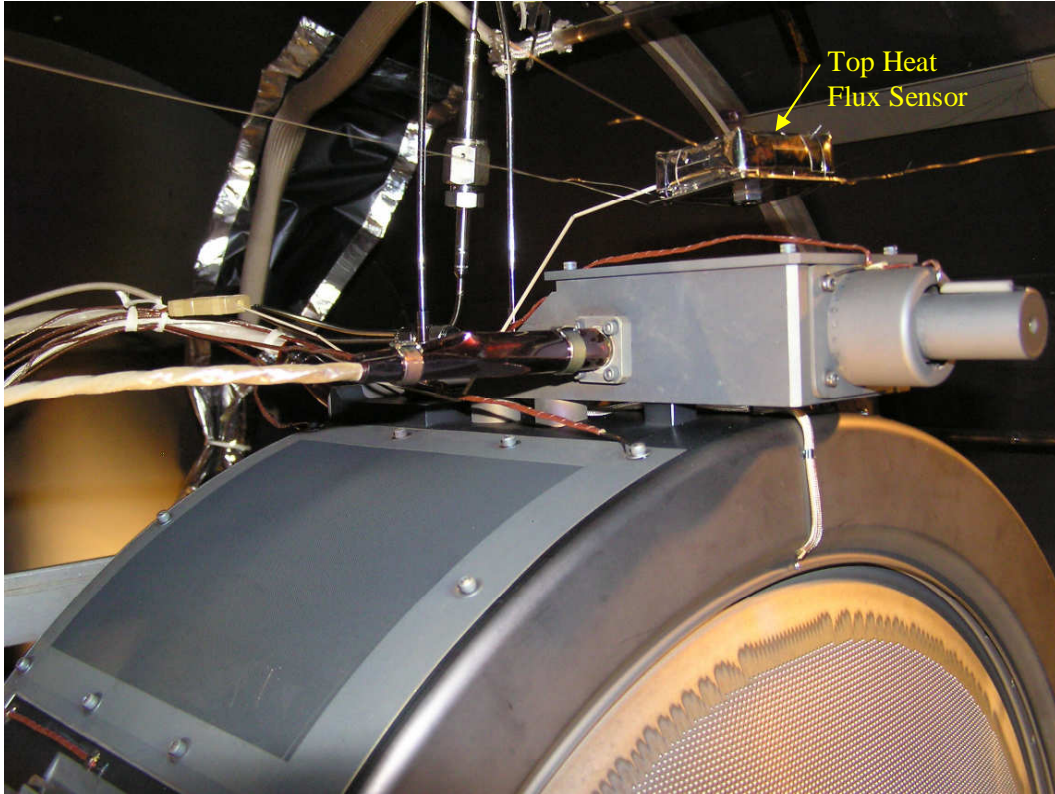


**Figure 3. NEXT PM1 Neutralizer and Top Heat Flux Sensor.**

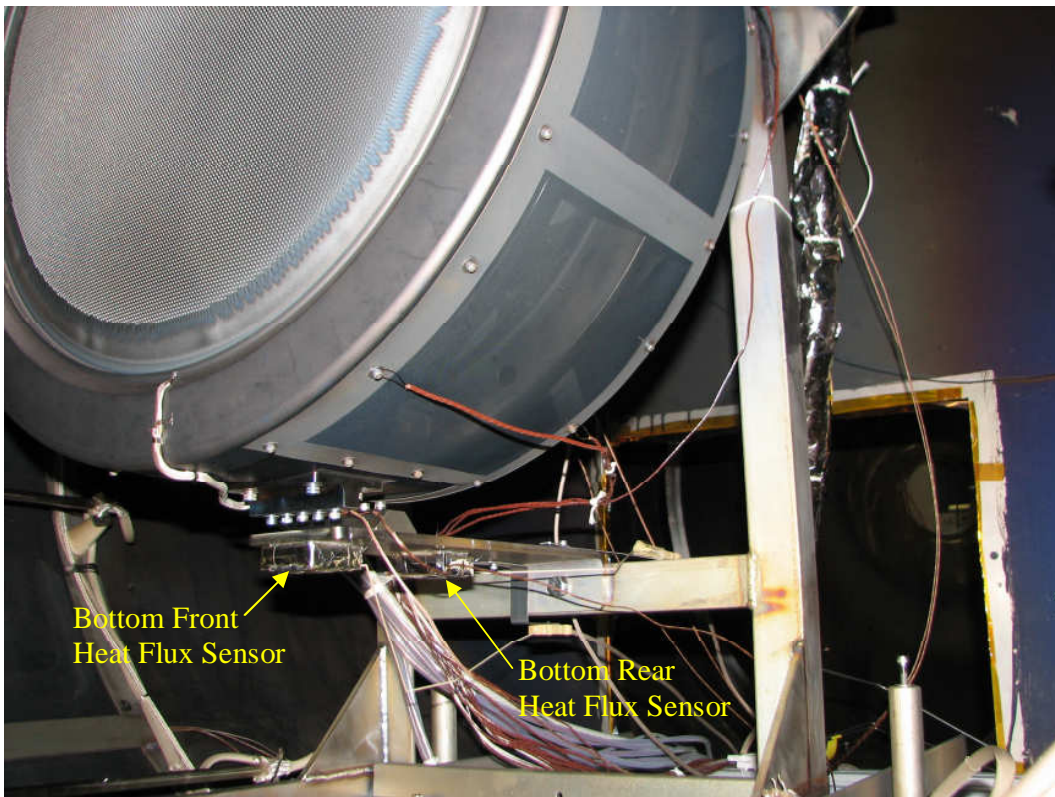


**Figure 4. NEXT PM1 and Bottom Heat Flux Sensors.**

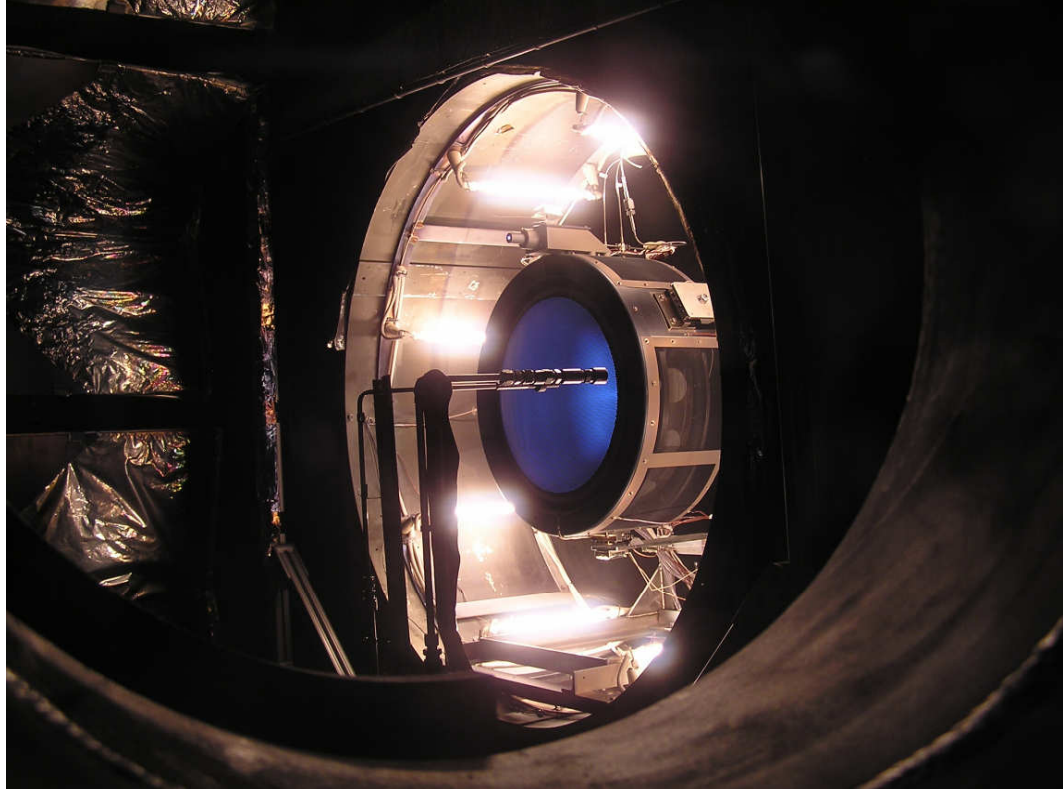


**Figure 5. NEXT PM1 in Shroud with Heat Lamps Operating.**

The shroud was equipped with a door made of multi-layer insulation. This door was opened during thruster operation; however, it could be closed to minimize thermal interaction with the vacuum facility during cold soak or hot soak when the thruster was not operating.

In addition to the shroud thermocouples other facility temperatures were monitored during the thermal development test. Thermocouples were located behind the graphite liner at the downstream end of the vacuum chamber as well as additional thermocouples on the side wall, on the ExB probe structure and on the cryopumps. Facility thermocouple locations, excluding those on cryopumps, are tabulated in Table 4.

**Table 4. Facility Thermocouple Locations.**

Thermocouple	Vacuum Chamber Component	Clocking	Axial Distance From PM1 (Side Wall) Distance From Vacuum Chamber Centerline (Other TCs)
ExB Shield Plate	ExB Probe Stand	3	0.12 m
ExB Motor Shield	ExB Probe Stand	9	0.08 m
ExB Base Plate	ExB Probe Stand	6	0.09 m
Beam Dump Chevron	Back Wall	10	0.63 m
Side Wall Back	Side Wall	4	4.5 m
Side Wall Middle	Side Wall	4	3.0 m

Double-to-single ion current ratios could be measured by an ExB probe mounted in the chamber 5.1 m downstream of the thruster. The ExB probe was aligned so that the probe collimator accepted beam ions from a 0.1 m diameter region at the center of the thruster.

Beam current density profiles could be measured by two Faraday probes. The Faraday probes were installed on a stage that allowed them to translate through the thruster plume at axial distances between 0.045 m and 0.55 m downstream of the thruster. One probe was supplied by GRC and the other was provided by JPL; the probes will be referred to as the GRC or JPL probe.

The probes were mounted 8.7 cm apart and aligned so that they sweep through the same plane when they collect ions. Both probes collected ion current on a circular button which was surrounded by a guard ring. The GRC probe button had a 1 cm square active area while the JPL probe button had a 0.21 cm square collection area. Both probes had guard rings surrounding the current collection buttons. The GRC probe had a 1.2 mm gap between the button and the guard ring, while the JPL probe had a 0.3 mm gap. The GRC probe guard ring had an outer diameter of 22.2 mm, compared to an outer diameter of 9.7 mm for the JPL probe. For the JPL probe both the button and guard ring were biased at -30 V during data collection. The GRC probe button was biased at -30 V and in most cases the guard ring was grounded (although a few traces were obtained with the guard ring biased at -30 V) while data was taken.

Figure 5 is a photograph taken through a side port in the vacuum chamber. Seen in the photograph is NEXT PM1 operating in the shroud with heat lamp power applied. Also visible in front of the thruster are the two Faraday probes.

### III. Functional Testing

A performance verification test was conducted prior to initiating the functional testing. This test was performed to verify that the thruster operated properly over its throttle range. The thruster was operated at four points; discharge only, 1.00 A 275 V, 2.00 A 1179 V and 3.52 A 1800 V. The thruster operated nominally at all points.

Functional testing was performed to verify engine performance, characterize the neutralizer, measure electron backstreaming and perveance margins, determine double-to-single ion current ratios and characterize the beam current density profile. This testing was performed prior and subsequent to the thermal development test.

No significant variation in thruster operating parameters was observed between the pre-TDT and post-TDT functional testing, indicating that the thruster did not suffer any adverse effects from the thermal development test.

The vacuum chamber pressure was higher during some of the post-TDT functional testing than it was for the pre-TDT functional test. This occurred because the graphite panels lining the vacuum chamber outgas when heated after exposure to atmosphere. Most of the outgassing occurred the first time the panels were heated by the ion beam from the thruster. The panels were outgassed during thruster performance verification testing prior to initiating the pre-TDT functional. The vacuum chamber was exposed to atmosphere immediately prior to the start of the post-TDT functional. The graphite panels were outgassed during the course of post-TDT functional testing. Vacuum facility pressure directly influenced accelerator grid currents and contributed to variations in discharge conditions.

#### A. Test Data

During performance testing all thruster currents, voltages and flow rates were recorded. Vacuum chamber pressure, vacuum facility and shroud temperature measurements were also stored. All thruster thermocouples, except the gimbal pad temperatures, were recorded during the pre-TDT performance test. The gimbal pad thermocouples were connected to the data acquisition system prior to the start of the thermal development test. After the TDT was concluded all thruster thermocouples, except those on the front mask and gimbal pads, were removed. The front mask and gimbal pad temperatures were recorded during the post-TDT functional testing.

#### B. Neutralizer Characterization

Neutralizer characterization is performed by decreasing the neutralizer flow rate until the neutralizer transitions from spot to plume mode. Plume mode is characterized by electrical oscillations in the neutralizer keeper circuit. Plume mode is defined as reaching or exceeding 5 V peak-to-peak oscillations measured between neutralizer keeper and neutralizer common. The neutralizer characterization was performed by lowering the flow rate to a minimum value or until the 5 V peak-to-peak oscillations occurred. During these tests the discharge was operating at 9 A current and the high voltage was turned off. To avoid picking up spurious noise, the peak-to-peak oscillations were measured across the neutralizer keeper power supply and not on the sense lines returning from the thruster.

During both the pre- and post-TDT functional testing the neutralizer did not reach the 5 V peak-to-peak criteria because the minimum flow rate was reached first. During the pre-TDT characterization the minimum flow rate was 2.5 sccm where the oscillations reached 4.2 V peak-to-peak. In the post-TDT functional the minimum flow rate was 2.9 sccm where the oscillations were 3.4 V peak-to-peak. The two tests showed similar trends although the neutralizer keeper voltage was between 1 and 2 V lower during the post-TDT test and the oscillations were larger at higher flow rates during the pre-TDT functional. Plots of the neutralizer characterization data appear in Figures 6 and 7. Figure 6 shows the time averaged neutralizer keeper voltage and Figure 7 shows the magnitude of the peak-to-peak voltage oscillations.

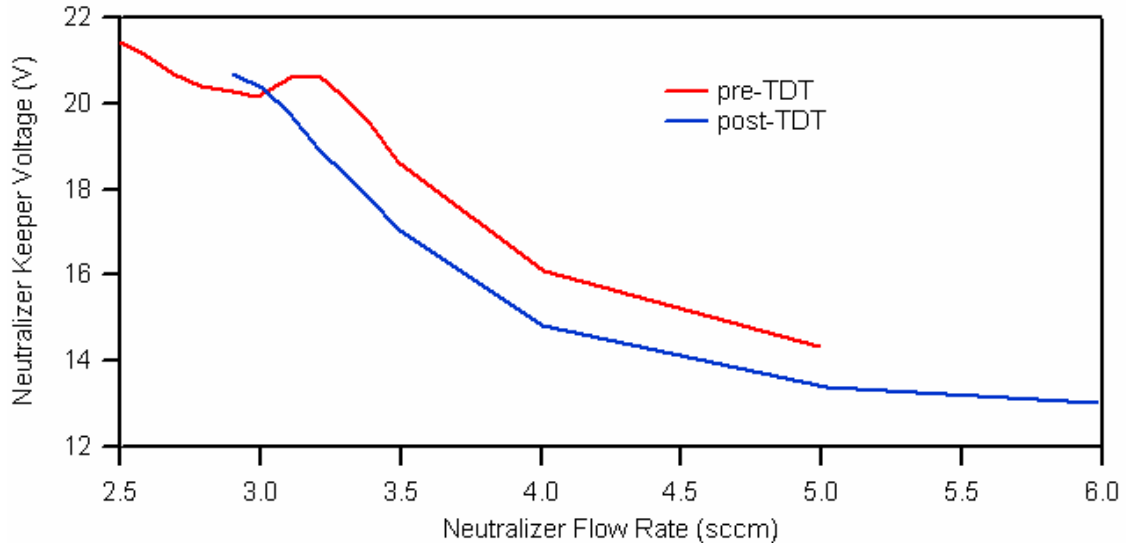


**Figure 6. Neutralizer Characterization Data**

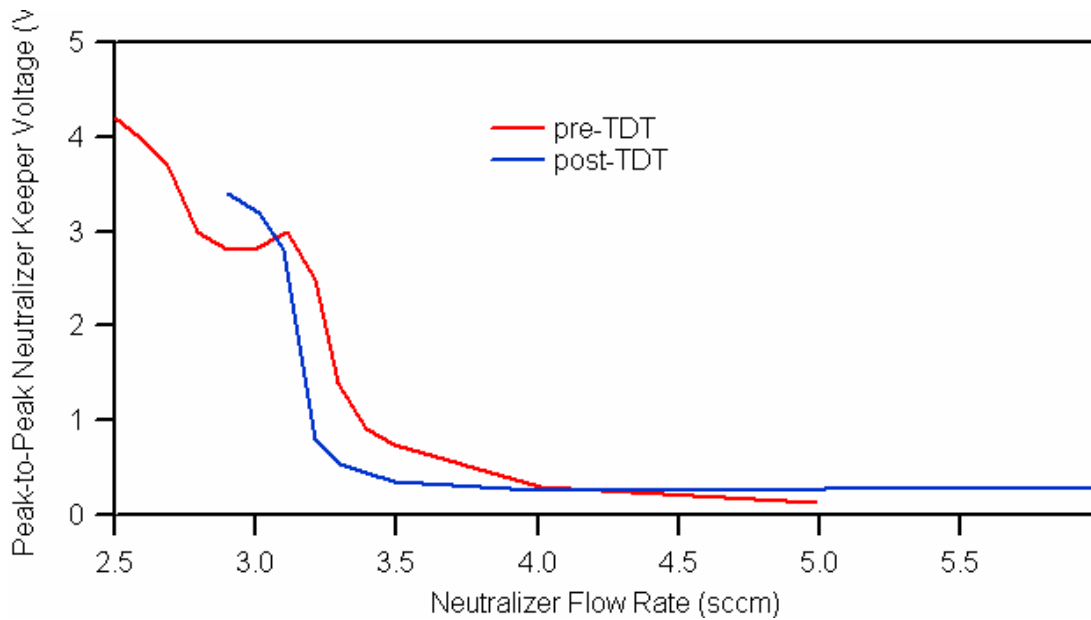


**Figure 7. Neutralizer Characterization Oscillation Data**

### C. Optics and ExB Data

During functional testing two measurements—perveance limit and electron backstreaming limit—related to the ion optics system were made. In addition ExB probe data were obtained to determine the double-to-single ion current ratio extracted from the thruster.

The perveance limit is measured by defocusing the ion beam until ions directly impinge on the accelerator grid. Defocusing is accomplished by reducing the screen grid voltage. The perveance limit is defined as the screen grid voltage at which a 0.02 mA increase in accelerator grid current is caused by a 1 V decrease in screen grid potential.

Electron backstreaming occurs when the potential at the center of accelerator grid apertures is insufficiently negative to preventing electrons from traveling upstream into the discharge chamber. Both electrons traveling upstream into the discharge chamber and positive ions traveling downstream are measured as positive current; when electron backstreaming occurs the indicated beam current increases. During the electron backstreaming tests beam control was disabled and the discharge current was maintained at a constant value. Initially the beam current

decreases slightly because the electric field between the grids decreases as the accelerator grid voltage increases. However, when the accelerator grid potential increases to the point that electron backstreaming begins the indicated beam current begins to increase. The electron backstreaming limit is determined by raising the accelerator grid voltage until the indicated beam current increases by 1 mA.

The double-to-single ion current ratio is measured using the ExB probe with the collimator viewing the center of the NEXT PM1 optics. The measured ratio is corrected for charge exchange losses<sup>9</sup> while the beam traverses the distance between the thruster and the probe. This was done by assuming the pressure was constant throughout the vacuum chamber and integrating the loss of double and single ions, due to charge-exchange with neutrals, over the distance between the thruster and the probe.

Perveance limit, electron backstreaming limit and ExB probe data for the pre-TDT and post-TDT functional testing is tabulated in Table 5. The variation in the pre-TDT and post-TDT perveance and electron backstreaming limits are within typical experimental scatter. This indicates that no significant changes to the ion optics occurred during the thermal development test. The ExB data do not vary appreciably between the two functional tests.

Table 5. NEXT Functional Test Flow Perveance Limit, Electron Backstreaming Limit and ExB probe Data

Functional Test Case	Perveance Limit (V)	Electron Backstreaming Limit (V)	Double to Single Ion Current Ratio
Pre-TDT Cases:			
1.2 A, 679 V	452	-49	
2.0 A, 1179 V	486	-100	0.07
3.52 A, 1800 V	612	-162	0.05
Post-TDT Cases:			
1.2 A, 679 V	457	-47	0.07
2.0 A, 1179 V	488	-96	0.07
3.52 A, 1800 V	593	-156	0.04
3.52 A, 1800 V	603	-157	
3.52 A, 1800 V	638	-158	0.05
3.52 A, 1179 V	647	-137	0.07

#### D. Beam Current Profiles

Beam current density profiles were obtained with the GRC and JPL faraday probes. The guard ring on the JPL probe was biased to -30 V while beam profiles were taken. To compare results from previous testing the GRC probe guard ring was held at ground potential during most tests; for a few test cases it was also biased at -30 V.

Typical plots of the Faraday probe traces comparing pre-TDT and post-TDT testing are shown in Figures 8 and 9 for the GRC and JPL probes. These traces were obtained with the probes 4.5 cm downstream of the accelerator grid. The beam current density traces were numerically integrated for comparison with the thruster beam current. The integration was performed using the trapezoidal rule after subtracting off the baseline current density from the probe data. The base line current was determined from the current collected when the probe was outside of the beam.

The integrated current for both probes tended to be high. The JPL probe integrated current tended to be about 5 to 10% greater than the beam current produced by the thruster. When the GRC probe guard ring was biased at -30 V the integrated current was between 15 and 30% high; however, when the GRC probe guard ring was biased at 0 V the integrated current was about 5 to 20% high. Although the reason for the difference is not known another trend in the Faraday probe data is noted; for traces taken before the post-TDT functional, at 4.5 cm between the probe and the optics, the integrated current is higher for both the GRC and JPL probes than it was for the post-TDT functional. For the post-TDT functional the integrated beam current for both probes were still high but within 4% for the 3.52 A beam current cases. This trend is noted for both the 1179 and 1800 V cases. The difference does not appear to be accounted for by variation in charge exchange ion collection due to tank pressure differences. For the 1179 V cases the post-TDT pressure was lower than the earlier run, while for the 1800 V cases the post-TDT pressure was comparable or higher than for the previous data.

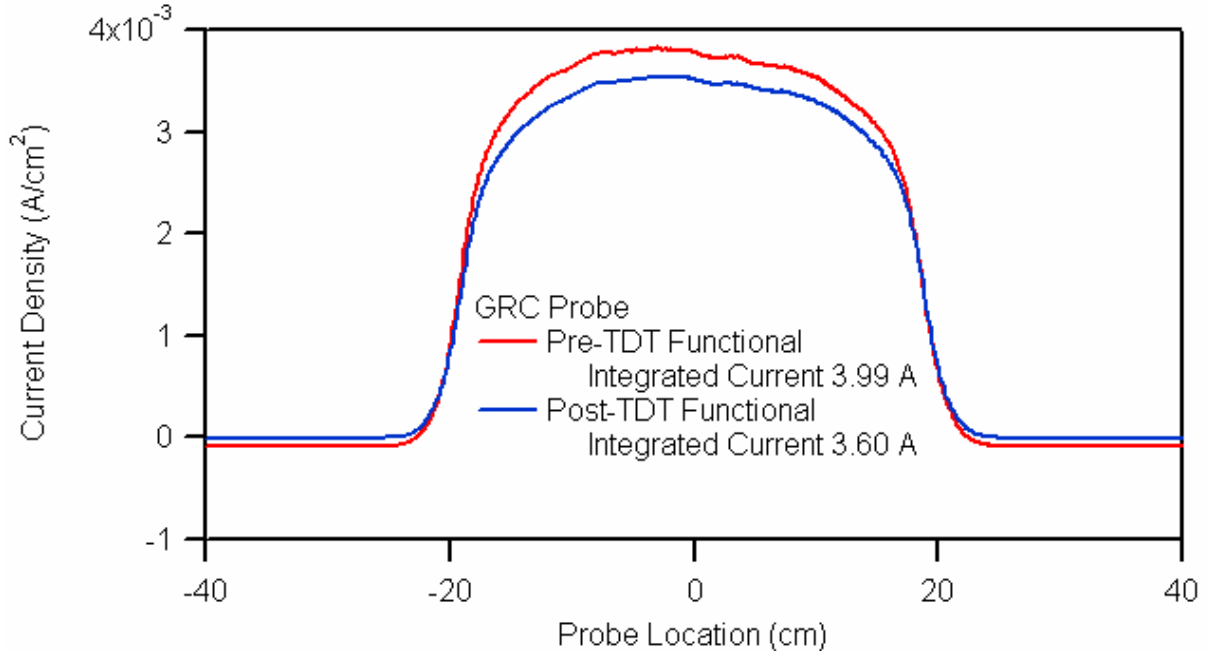


**Figure 8. Comparison of Pre- and Post-TDT Functional Faraday Probe Data at 1800 V, 3.52 A**

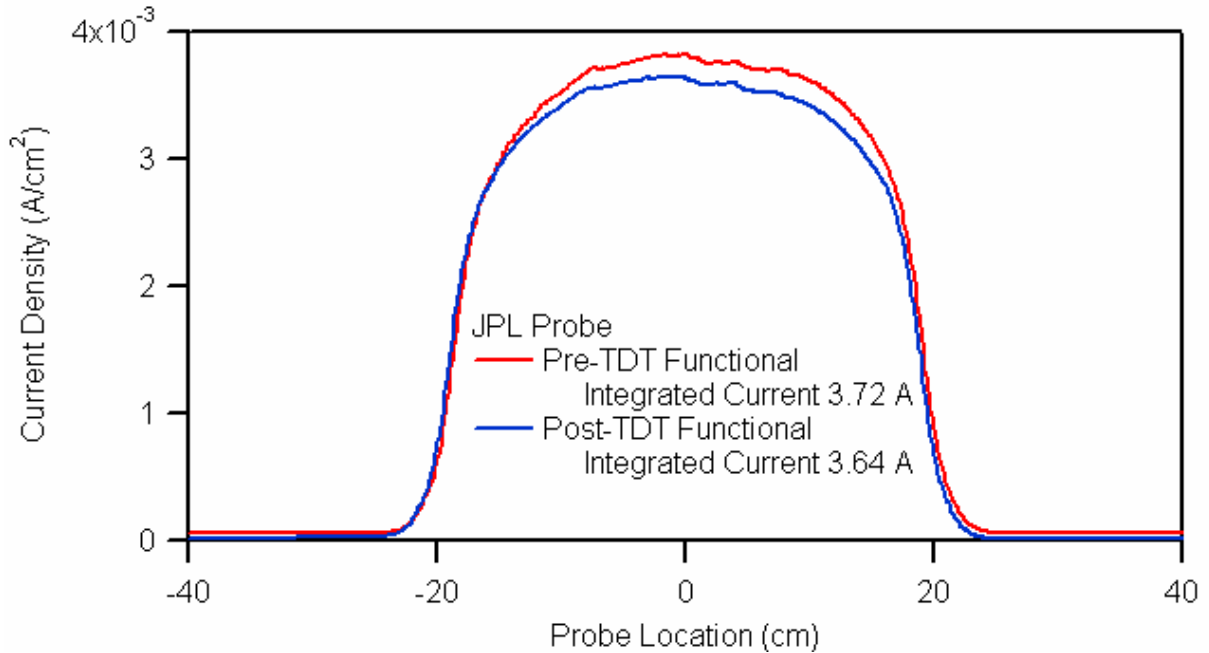


**Figure 9. Comparison of Pre- and Post-TDT Functional Faraday Probe Data at 1800 V, 3.52 A**

Faraday probe sweeps were obtained at axial distances from the optics ranging from 4.5 cm to 0.53 m. At distances greater than  $\sim 0.35$  m the integrated current tends to decrease indicating that the probes may not have swept far enough radially to collect the most divergent ions.

Beam divergence estimates were obtained from the Faraday probe data. The radius that contained 0.95 of the beam was determined from the integration of the beam current. The active grid radius of 0.18 m was subtracted from the beam radius and dividing by the axial distance between the optics and the Faraday probe gave the tangent of the beam divergence angle. Due to grid dishing the outer edge of the active area of the grid is located 0.023 m further from the probe than the grid center; this additional axial distance is accounted for in computing the beam divergence angle. Both probes give comparable results for the divergence angle. At full power (3.52 A, 1800 V) the divergence

angle was estimated to be in the range of 17 to 20°. At 3.52 A, 1179 V the divergence angle was about 13°. At 2.00 A, 1179 V the divergence angle was about 16°. At 1.20 A, 679 V the divergence angle was approximately 14°. Plots showing the divergence data obtained during the post-TDT testing is shown in Figures 10 and 11.

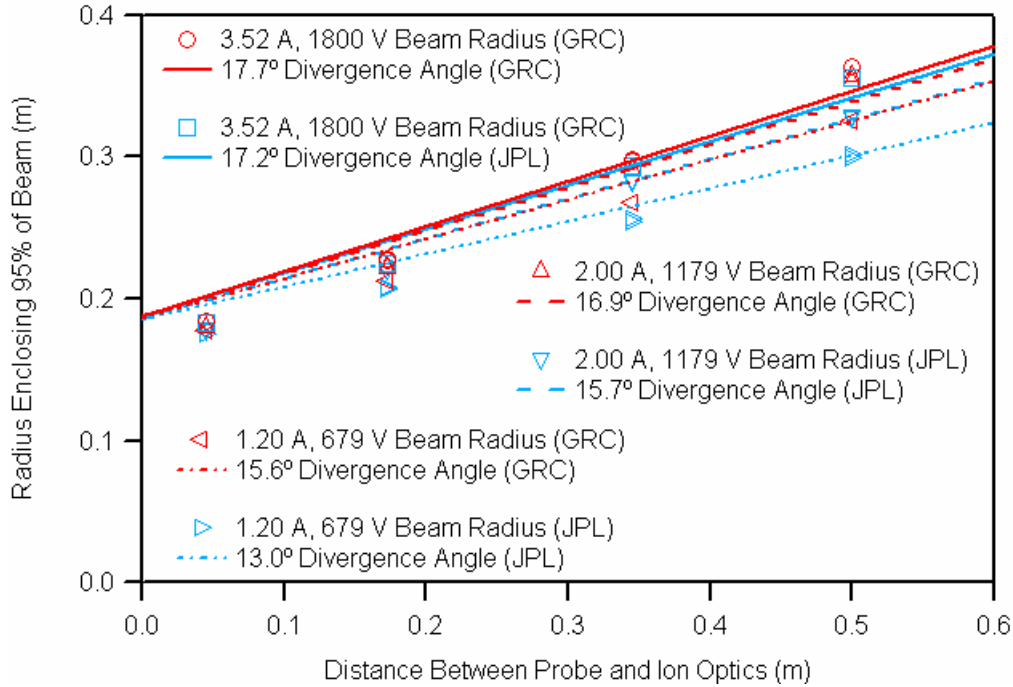


**Figure 10. Beam Divergence During Post-TDT Functional**

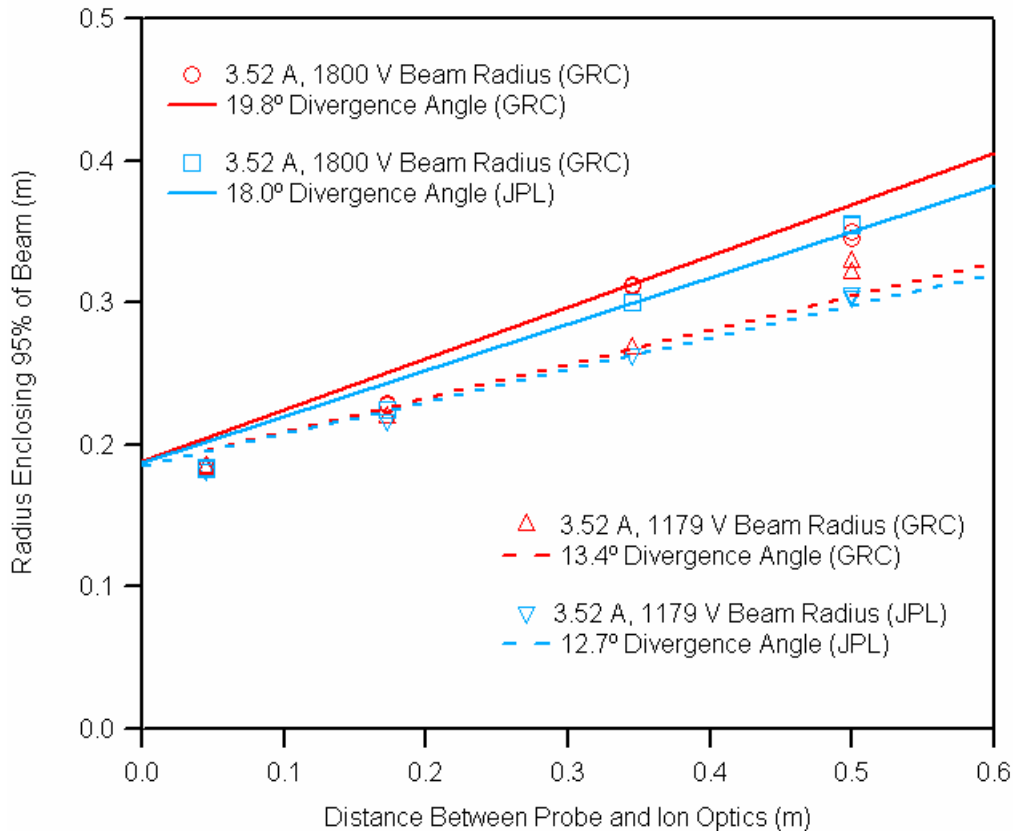


**Figure 11. Beam Divergence During Post-TDT Functional**

### E. Cathode Ignition

During functional testing the thruster cathodes (neutralizer and discharge cathode) were started by operating their heaters at 8.5 A until the cathode ignited; once the cathode ignited the heater power was turned off. Flow to the cathode was initiated between 2 to 3 minutes after the heater was turned on. At 3 minutes and 30 seconds the keeper supply was enabled in order to start the cathode; for the discharge cathode the discharge supply was also enabled. The test was conducted without high voltage pulse igniters. The open circuit voltage for the neutralizer keeper power supply was 150 V; the discharge cathode keeper supply open circuit voltage was 150 V and the discharge power supply open circuit voltage was 40 V.

Cathode ignition times are plotted in Figures 12 and 13; ignition time is the elapsed time between starting the cathode heater and the cathode igniting. Because the cathode keeper power was applied at 210 seconds this is the minimum ignition time. During functional testing the thruster was started nine times. Six of the starts were initiated with the thruster at ambient temperatures and three were performed after the thruster had been operating and the cathodes were still hot.

The neutralizer ignition time during the ambient starts ranged from 210 to 265 seconds and during the three hot starts the neutralizer ignited immediately at 210 seconds. The discharge cathode did not start as easily as the neutralizer. Ignition time during the ambient starts ranged from 265 to 547 seconds; for the hot starts it took between 210 and 282 seconds to start.

During acceptance testing at GRC, problems with igniting the PM1 discharge cathode was observed. The ignition times were erratic and varied from 270 s to over 1800 s. Due to the long ignition times the discharge cathode was reworked and tested at GRC prior to shipping to JPL. After the rework the discharge cathode ignition times varied between 270 and 360 s during testing conducted at GRC. Testing at GRC was conducted using a pulse igniter circuit that provided 750 V pulses between the keeper and cathode common. The pulse igniter circuit was not used during the pre- and post-TDT functional testing at JPL; the maximum cathode keeper to cathode common voltage was the 150 V open circuit provided by the keeper power supply. The difference in cathode start procedure is thought to account for the longer ignition times observed during testing at JPL.

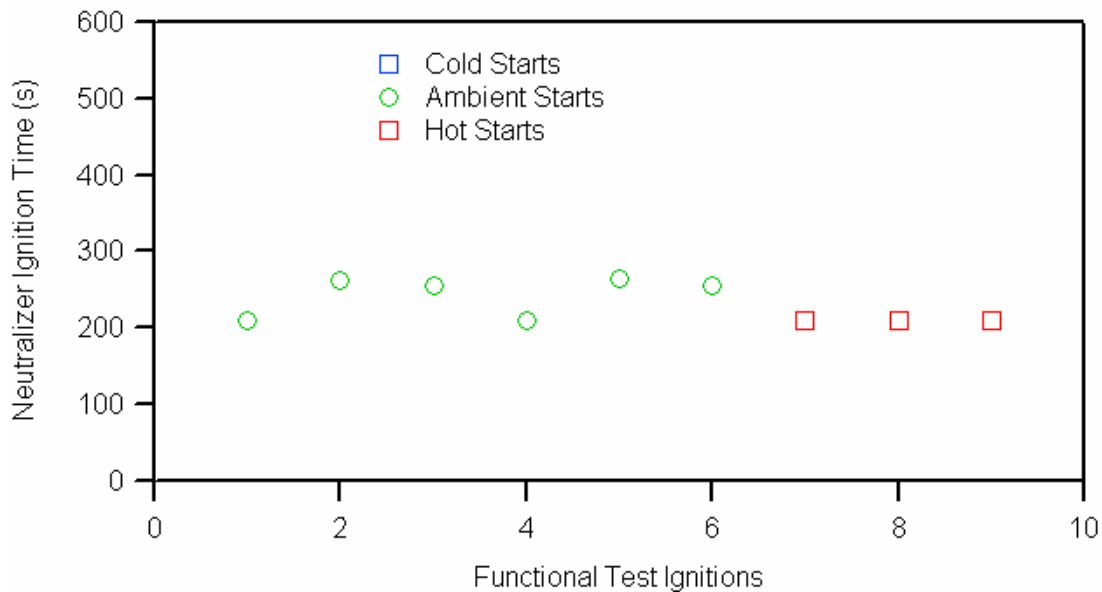
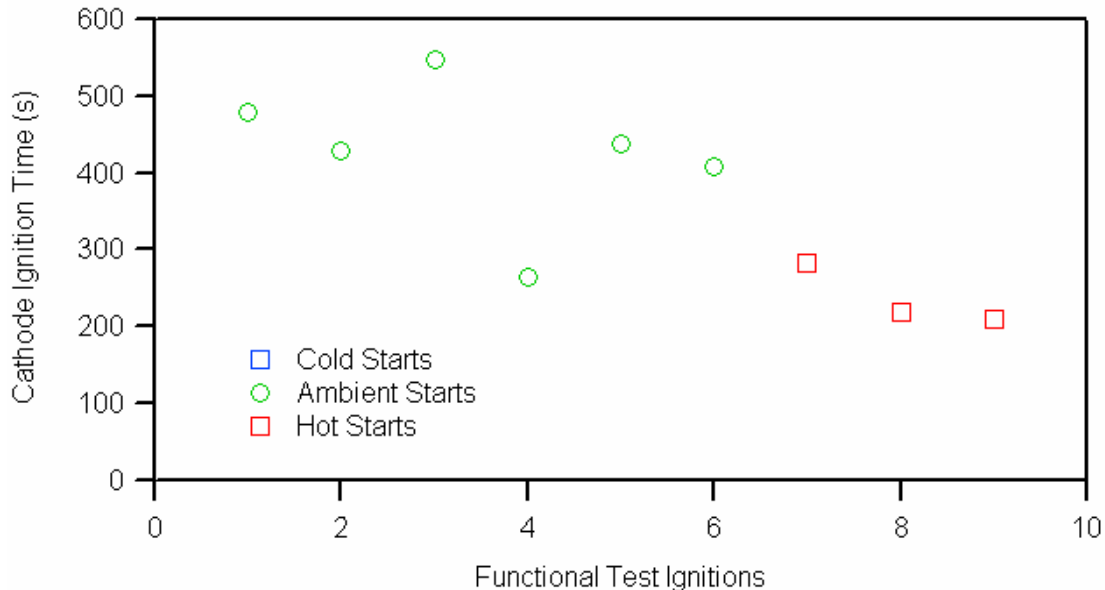


Figure 12. Neutralizer Ignition Time During Functional Testing



**Figure 13. Discharge Cathode Ignition Time During Functional Testing**

#### IV. Thermal Testing

Thermal testing was conducted at cold (liquid nitrogen cooling the shroud), ambient (no active external heating or cooling) and hot (heat lamps radiating to thruster and shroud) conditions. These tests encompassed the range of thermal conditions expected during a typical mission. An additional test was performed to determine the external heat flux required to reach the do not exceed temperature limit of the thruster or thruster component with the thruster operating at full power.

Steady state temperature data obtained during thermal testing is listed in tables found in the Appendix. These tables list the cold cases, then the ambient cases and the hot cases that were tested. The left column gives the thruster operating conditions and for the hot cases the coupon set point temperature used to control the lamps. Also listed in the Appendix are tables with the thruster operating parameters and facility parameters at the time when the thruster reached the steady state temperatures. The thruster was deemed to have reached steady state when the rate of temperature change for all thruster thermocouples was less than 4 C per hour.

A specific spacecraft configuration for mounting NEXT has not been identified yet; therefore, the boundary conditions for the NEXT thermal model have not been determined. In spaceflight the heat flux from the sun would heat one side of the thruster while the other side would radiate toward deep space. The spacecraft would also provide thermal interaction with the thruster. The experimental set up is different from that expected in space because the heat lamps were evenly spaced around the cylindrical portion of the thruster. As a result the entire cylindrical section was heated instead of just one side.

An analysis performed by GRC estimated the maximum solar heat flux to NEXT during potential missions. This estimate was based on the maximum solar heat flux found in a deep space design reference mission (DSDRM) analysis performed by Aerojet. This maximum solar heat flux, 1400 W/m<sup>2</sup>, occurs with the thruster operating at 0.85 AU at a sun angle of 38 degrees. Multiplying the heat flux by the projected area of the thruster illuminated by the sun the total solar power radiated to NEXT was estimated to be 450 W.

Because the spacecraft configuration has not been defined and because the heat lamps surround the thruster, the total radiated heat load to the thruster from the heat lamps and the shroud is used in this report. During hot testing radiated heat loads between 650 and 1000 W were applied to the thruster.

Overall the thruster operated well; however, there were two situations where instrumentation problems occurred. There was a problem with thermocouples arcing during hot testing when the thruster was operating at full power (3.52 A, 1800 V). There was also a problem with the data acquisition system during the neutralizer heater cold soak test. In both cases the steady state criterion (less than 4 C per hour rate of temperature change) was not achieved.

During hot testing at full power (3.52 A, 1800 V throttle point) continuous arcing was observed on the two occasions this test was attempted. The first time this occurred the cause was overheating of Teflon thermocouple insulation on the cylindrical magnet located at about the 8 o'clock (H2b). Volatiles evolving from the insulation

raised the local pressure until arcing between the thermocouple and the plasma screen occurred. Testing was interrupted, the vacuum facility was vented and the offending thermocouple was removed from the thruster. Several other thermocouples that were also located near the cylindrical magnet were wrapped in tantalum foil in an attempt to avoid any further arcing. Testing at full power under hot conditions was reattempted and again continuous recycling occurred as the thruster neared steady state. Post-TDT examination of the thruster did not reveal an obvious cause for the continuous recycling during the second attempt; however, it is suspected that the thermocouples were at fault. During the subsequent thermal vacuum test, with the thermocouples removed, the thruster was operated under hot conditions at full power without arcing giving further indication that the thermocouples caused the breakdown observed during the thermal development test.

During the neutralizer heater cold soak test segment problems with the data acquisition system were experienced resulting in loss of communication with the control computer. When communications are interrupted the system is set up to turn off all thruster power supplies. Although the thruster had not reached steady state, the test was not repeated because the results indicate that the neutralizer heater alone cannot be used to heat the thruster.

### **A. Heat Flux Estimation**

The radiated heat flux to the thruster is estimated by using the calibration and the temperature of the heat flux coupons at steady state thermal conditions. The area of the cylindrical portion of the thruster is  $0.33 \text{ m}^2$ , the area of the conical section is  $0.23 \text{ m}^2$ , and the area of the optics and front mask is  $0.21 \text{ m}^2$ . At steady state the coupon and shroud temperatures are comparable in the region with the heat lamps which surround the cylindrical portion of the thruster, suggesting that the shroud temperature could be used along with the heat flux sensor calibration to estimate the heat flux to the thruster. The temperature at the back of the shroud, which interacts with the conical section of the thruster, tend to be lower than the shroud temperatures surrounding the cylindrical section of the thruster; therefore, the heat flux to the thruster is lower in the conical region than in the cylindrical portion of the thruster. The temperature of the chamber interacting with the optics and front mask varies depending on where the ion beam is depositing power. Because the emissivity of the vacuum chamber surfaces is likely to be lower than that of the shroud the radiation to the optics and from mask was assumed to be black body at a temperature of 25 C. Portions of the vacuum chamber under direct beam impingement can reach temperatures approaching 100 C; however, the 25 C temperature will be used to provide a conservative estimate of the heat flux to the thruster.

The heat flux to the thruster at three operating conditions is estimated. The cases are at ambient with the thruster operating at full power, and two hot cases with the thruster operating at beam conditions of 3.52 A, 1179 V and the heat lamp set point at 100 C and 145 C.

At ambient full power operation (3.52 A, 1800 V) the coupon temperatures were 61 and 63 C, the back of the shroud was  $\sim 56 \text{ C}$ , and the vacuum chamber temperature was 25 C. Using these temperatures and the coupon calibration multiplier, the estimated total heat flux to the thruster operating at full power at ambient conditions is 450 W.

For the thruster operating at 3.52 A, 1179 V with the heat lamp set point at 100 C, the heat flux coupons were at 100 C, the back of the shroud was at about 90 C and again using at vacuum chamber temperature of 25 C, the estimated heat flux to the thruster was 650 W.

The highest heat flux case during the thermal development test was conducted with the heat lamp set point at 145 C and the thruster operating at beam conditions of 3.52 A, 1179 V. For this case the coupon temperatures were 144 C, the back of the shroud was at 134 C and once again the vacuum chamber temperature of 25 C is used. For this case the total heat flux to the thruster is estimated to be 1000 W.

### **B. Cathode Ignition**

During thermal development testing the neutralizer and discharge cathode were started by operating the heater at 8.5 A until the cathode ignited; once the cathode ignited the heater power was turned off. Flow to the cathode was initiated between 2 to 3 minutes after the heater was turned on. At 3 minutes and 30 seconds the keeper supply was enabled in order to start the cathode; for the discharge cathode the discharge supply was also enabled. The test was conducted without high voltage pulse igniters. The open circuit voltage for the neutralizer keeper power supply was 150 V; the discharge cathode keeper supply open circuit voltage was 150 V and the discharge power supply open circuit voltage was 40 V.

Cathode ignition times are plotted in Figures 14 and 15; ignition time is the elapsed time between starting the cathode heater and the cathode igniting. Because the cathode keeper power was applied at 210 seconds this is the minimum ignition time. During thermal development testing the thruster was started six times. Two of the starts were initiated with the thruster at cold temperatures, three with the thruster at ambient temperatures and one was performed after the thruster had been operating and the cathodes were still hot.

The neutralizer ignition time during the cold starts were 270 and 320 seconds. During ambient starts neutralizer ignition times ranged from 215 to 270 seconds. For the hot start the neutralizer ignited immediately at 210 seconds. As with the functional test starts the discharge cathode did not start as easily as the neutralizer. Ignition times during cold starts were 295 and 525 seconds. The ignition times for the ambient cathode starts ranged from 270 to 525 seconds. During the hot start the discharge cathode ignited immediately at 210 seconds.

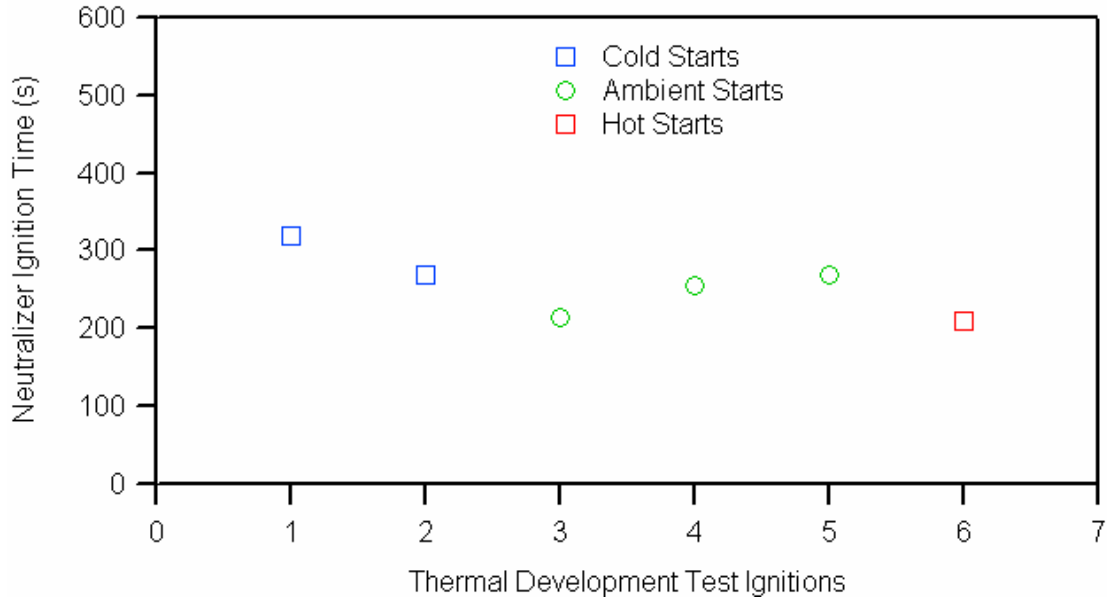


**Figure 14. Neutralizer Ignition Time**

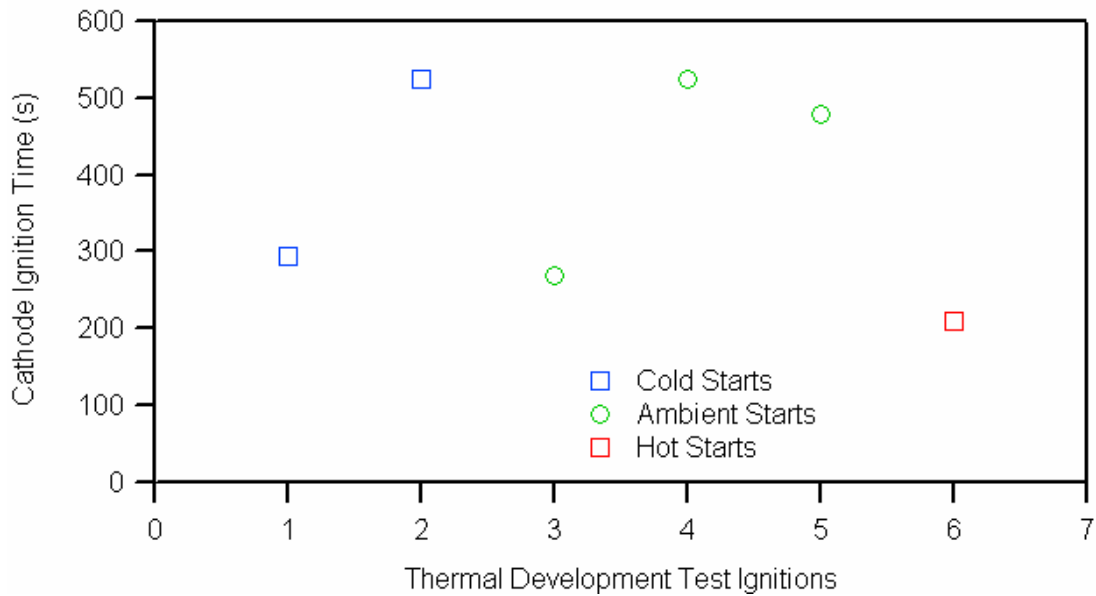


**Figure 15. Discharge Cathode Ignition Time**

As noted earlier during ambient testing at GRC, the reworked PM1 discharge cathode ignition times ranged from 270 to 360 s. The longer ignition times observed at JPL were likely due to the fact that a pulse igniter circuit—used during GRC testing—was not used during the thermal development test.

### C. Cold Testing Results

The data from the cold case using the cathode heater at a current of 7.2 A indicate that the discharge cathode heater is capable of maintaining the magnets at temperatures greater than 0 C and the harnesses and propellant isolators at temperatures greater than -30 C while the shroud was cooled with liquid nitrogen. The gimbal pads—used as the candidate reference temperature locations—were also maintained at temperatures greater than -30 C.

As would be expected, temperatures were higher when the thruster was operating. For the two cold cases with the thruster operating at beam conditions of 3.52 A, 1179 V and 3.52 A, 1800 V the magnet temperatures were in the 190 to 235 C range. The neutralizer keeper reached temperatures between 550 and 560 C; the discharge cathode assembly tube temperatures ranged between 455 and 470 C. The harness temperatures ranged between 115 and 165 C and the gimbal pads ranged from 115 to 145 C.

The thruster was more susceptible to recycling during cold testing than during normal operation at ambient and hot conditions (excluding the continuous recycling at full power hot conditions). Due to a timing problem the recycle counter captured some but not all recycles so the absolute recycle rate could not be determined; however, the relative rate was higher during cold testing when the high voltage was first applied and the rate decreased as the thruster warmed up. Although it dropped some the recycle rate continued to stay higher than during ambient or hot operation as long as the shroud was actively cooled.

As noted earlier all cold test cases except the neutralizer heater cold soak case reached steady state. For this neutralizer case fifteen thermocouples indicated a rate of temperature change greater than 4 C per hour. Of the fifteen all but five were below 4.5 C per hour. The thermocouples that measured rates of change greater than 4.5 C per hour were the accelerator grid support (H12) at 6.2 C per hour, the neutralizer support temperature (L2) at 6.4 C per hour, the gimbal pad at the 2 o'clock location (L6) at 6.3 C per hour, the plasma screen cone/conical interface (L8) at 7.8 C per hour and the harness near the neutralizer exit (L9) at 6.2 C per hour. These data are tabulated in the Appendix.

#### **D. Ambient Testing Results**

The ambient cases provided thermal data over the thruster operating range; these data are primarily useful for validating the thermal model. The thruster operated nominally at all ambient conditions tested. The thermocouple instrumentation provided one interesting piece of information; when the thruster was transitioned from 3.52 A, 1179 V to 3.52 A, 1800 V, the cylindrical magnet thermocouple temperatures increased between 6 and 15 C while the other magnet temperatures remained essentially unchanged. Although this could be due to a change in the distribution of power in the discharge chamber, it is more likely due to electron backstreaming through the plasma screen when the beam voltage is increased from 1179 V to 1800 V. It is believed that such electron backstreaming caused the failure of the thermocouple insulation that caused the arcing observed during hot testing. The highest temperature observed during ambient testing was the 255 C cylindrical magnet temperature observed during operation at full power (3.52 A, 1800 V).

#### **E. Hot Testing Results**

Testing using the lamps to apply an external heat load to the thruster was performed to provide data to validate the thermal model and to determine temperature margins when external heat loads ranging between 650 and 1000 W were input to the thruster.

In one case heat lamps were used to heat the thruster while it was not operating. The set point temperature for the lamp control coupon was 100 C. Because the lamps were located around the side of thruster and the shroud behind the thruster heated up when the lamps were applied, steady state temperatures along the side and back of the thruster were between 85 and 100 C. Temperatures on the front mask were about 50 C and the optics were between 65 and 80 C.

Hot operation of the thruster at 3.52 A, 1179 V and 3.52 A, 1800 V were performed. During operation at 3.52 A, 1800 V with the lamp control temperature set at 100 C, the thruster began to continuously recycle at it approached steady state on the two occasions where this test was attempted. In the first case failure of cylindrical magnet thermocouple was the cause. No definitive reason for the continuous recycling was identified for the second case; however, overheating of the thermocouples due to electrons backstreaming through the plasma screen is suspected. The thruster was able to operate with the same external thermal load at 3.52 A, 1179 V. The electric field between the plasma screen and the discharge chamber is weaker during operation at 1179 V than it is at 1800 V. Therefore, it is possible that backstreaming electrons during 3.52 A, 1800 V operation may have heated the thermocouples until they were close to their failure limit. The Teflon insulated thermocouples were rated to 260 C which the thermocouple was approaching when it failed.

Although these full power hot cases did not reach the steady state thermal criterion one case was relatively close; in the first attempt all except three thermocouples meet the criterion for steady state. The discharge chamber

thermocouple located at 7 o'clock (H5) measured a temperature rate of rise of 5.9 C per hour and the gimbal pad temperature at 2 o'clock (L6) was increasing at 4.4 C per hour. The third thermocouple that did not meet the steady state criterion was the one that failed which indicated the temperature was decreasing at over 30 C per hour as it was degrading. The data for this case are tabulated in the Appendix. In the second case of continuous arcing about half of the thermocouples were indicating temperature rates of change greater than the 4 C per hour criterion; because this case was not near steady state the data from this case is not tabulated in the Appendix.

The thruster was also operated at 3.52 A, 1179 V with the lamp set point at 145 C; this provided an estimated total external heat load of 1000 W to the thruster. Under these conditions the wire harness reached 220 C which was 10 C from its do not exceed temperature limit of 230 C. The magnets still had over 80 C margin since the highest temperature reached was 272 C. The propellant isolator margin was over 70 C as it reached an upper temperature of 193 C.

#### **F. Post-TDT PM1 Inspection**

The thruster was removed from the vacuum facility and placed in a clean room at JPL. The thruster was inspected and disassembled in the clean room. The remaining thermocouple wires for the discharge chamber and the magnets appeared to have gotten hot but no obvious signs of arcing were found.

With two minor exceptions the thruster was found to be in good condition during the post-TDT inspection. One thermocouple punched through the discharge chamber mesh when the thermocouple was being removed. The small hole in the discharge chamber wall was repaired by spot welding a tantalum foil patch to the outside of the discharge chamber.

The thruster was hypotted during the inspection and the impedances between thruster components were found to be nominal with the exception of cathode common to anode. The cathode common to anode impedance was 3.9 M $\Omega$  when it was first checked; after removing and reinstalling the wiring at the back of the discharge cathode assembly, the impedance had improved to 7.5 M $\Omega$ . Because the voltage between the anode and cathode common is less than 30 V during normal thruster operation, the observed impedance results in negligible leakage current and is not a concern unless it continues to decrease during subsequent operation.

### **V. Recommendations**

The major recommendation from the thermal development test is that the gimbal pads be used as the reference temperature location for the thermal vacuum test. It is desirable to have the reference thermocouples on low voltage surfaces in order to avoid problems with high voltage stand off; therefore, the gimbal pads and the front mask were the two candidates for the reference temperature locations. Based on thermal development test data and modeling done at GRC the gimbal pads were determined to provide a better correlation with critical components—such as the magnets, propellant isolators and wire harnesses—than the front mask. The heat lamps surrounding the cylindrical portion of the thruster do not have a direct view of the front mask; because of this the external radiated heat load does not couple well to the front mask. The gimbal pads, located on the cylindrical section of the thruster, view the heat lamps directly and their temperatures correlate well with the heat flux provide by the lamps. Therefore the gimbal pads are recommended for the reference temperature location.

Two other recommendations, based on the thermocouple problems observed during the test, are also given. In order to avoid having the instrumentation limit the externally applied heat load, the thruster should be instrumented with thermocouples capable of withstanding the highest “do not exceed” temperature. For NEXT this maximum is the 360 C specified for the magnets. It is also recommended that the plasma screen be modified to reduce or eliminate electron backstreaming through it. This can be accomplished by decreasing the size of the apertures in the screen. In addition, redesigning the screen surrounding the cylindrical section of the thruster as a solid piece should be considered.

### **VI. Summary**

The NEXT PM1 thruster was operated over a range of thermal conditions that bracket those that would be expected during a typical mission. Thermal conditions ranged from liquid nitrogen cooled shroud temperatures to 1000 W externally applied heat load. The data obtained during the test is useful for validating the thruster thermal model.

The thruster performed well during the thermal development test, although there was a problem with the thermocouples used during the test. For the largest external heat load of 1000 W to the thruster the harness temperature was within 10 C of its limit while the margin for the magnets and propellant isolator were over 70 C.

During cold testing it was determined that the cathode heater could be used to maintain the thruster at temperatures greater than -30 C. Use of the cathode heater could be considered instead of using an external heater on a spacecraft. If the cathode heater were to be used to provide auxiliary heating during a mission an analysis would be required to determine the probability of cathode heat failure due to performing this extra duty.

### Appendix

Steady state data for the four cold tests, eight ambient cases, and four hot thermal development test operating conditions are tabulated here. For these tests, steady state is defined as a temperature change less than 4 C per hour for all thruster thermocouples. As noted in the Thermal Testing section all cases—except the full power (3.52 A, 1800 V) hot case and the neutralizer cold soak heater case—reached the steady state condition during testing. Thermocouple and thruster currents, voltages, and flow rates are all listed for the thermal development test cases.

**Table 6. NEXT Thermal Development Test Neutralizer and Cathode Heater Data**

Thermal Case	Neutralizer Heater Current (A)	Neutralizer Heater Voltage (V)	Cathode Heater Current (A)	Cathode Heater Voltage (V)
Cold Cases:				
Neutralizer Heater (7.2 A, 8.7 V)	7.2	8.7	0.0	0.0
Cathode Heater (7.2 A, 13.7 V)	0.0	0.0	7.2	13.7
3.52 A, 1179 V	0.0	0.6	0.0	0.4
3.52 A, 1800 V	0.0	0.6	0.0	0.4
Ambient Cases:				
Discharge Only (9.1 A, 24.2 V)	0.0	0.3	0.0	0.1
1.0 A, 275 V	0.0	0.3	0.0	0.1
1.2 A, 679 V	0.0	0.4	0.0	0.2
1.2 A, 1179 V	0.0	0.4	0.0	0.1
1.2 A, 1800 V	0.0	0.4	0.0	0.1
2.0 A, 1179 V	0.0	0.5	0.0	0.2
3.52 A, 1179 V	0.0	0.7	0.0	0.4
3.52 A, 1800 V	0.0	0.7	0.0	0.4
Hot Cases:				
No Thruster Operation	0.0	0.0	0.0	0.0
100 C set point 3.52 A, 1179 V	0.0	0.7	0.0	0.5
100 C set point 3.52 A, 1179 V	0.0	0.7	0.0	0.5
145 C set point 3.52 A, 1800 V	0.0	0.7	0.0	0.4
100 C set point				

**Table 7. NEXT Thermal Development Test Flow Rate and Tank Pressure Data**

Thermal Case	Neutralizer Flow Rate (sccm)	Cathode Flow Rate (sccm)	Main Flow Rate (sccm)	Tank Pressure (Torr)
Cold Cases:				
Neutralizer Heater (7.2 A, 8.7 V)	0.00	0.00	0.00	3.0e-08
Cathode Heater (7.2 A, 13.7 V)	0.00	0.00	0.00	7.0e-08
3.52 A, 1179 V	4.02	4.86	49.53	5.6e-06
3.52 A, 1800 V	4.02	4.86	49.54	5.7e-06
Ambient Cases:				
Discharge Only (9.1 A, 24.2 V)	5.98	3.57	14.25	2.2e-06
2.0 A, 275 V	4.15	3.43	12.34	2.2e-06
1.2 A, 679 V	3.00	3.57	14.21	2.4e-06
1.2 A, 1179 V	3.00	3.57	14.24	2.6e-06
1.2 A, 1800 V	3.00	3.57	14.23	2.9e-06
2.0 A, 1179 V	2.49	3.86	25.82	3.5e-06
3.52 A, 1179 V	4.01	4.87	49.56	6.0e-06
3.52 A, 1800 V	4.01	4.87	49.58	7.0e-06
Hot Cases:				
No Thruster Operation	0.00	0.00	0.00	3.0e-08
100 C set point 3.52 A, 1179 V	4.01	4.86	49.60	6.5e-06
100 C set point 3.52 A, 1179 V	4.01	4.88	49.55	6.4e-06
145 C set point 3.52 A, 1800 V	4.01	4.86	49.55	6.0e-06
100 C set point				

**Table 8. NEXT Thermal Development Test Beam and Accelerator Grid Data**

Thermal Case	Beam Current (A)	Beam Voltage (V)	Accelerator Grid Current (mA)	Accelerator Grid Voltage (V)
Cold Cases:				
Neutralizer Heater (7.2 A, 8.7 V)	0.00	0	0.00	0
Cathode Heater (7.2 A, 13.7 V)	0.00	0	0.00	0
3.52 A, 1179 V	3.54	1174	21.33	-201
3.52 A, 1800 V	3.53	1800	24.48	-211
Ambient Cases:				
Discharge Only (9.1 A, 24.2 V)	0.00	0	44.45	0
3.0 A, 275 V	1.01	275	5.13	-500
1.2 A, 679 V	1.20	678	4.65	-115
1.2 A, 1179 V	1.20	1180	4.94	-200
1.2 A, 1800 V	1.20	1806	7.46	-210
2.0 A, 1179 V	2.00	1178	9.07	-200
3.52 A, 1179 V	3.55	1174	25.22	-201
3.52 A, 1800 V	3.50	1800	25.70	-211
Hot Cases:				
No Thruster Operation	0.00	0	0.00	0
100 C set point 3.52 A, 1179 V	3.52	1174	28.97	-200
100 C set point 3.52 A, 1179 V	3.51	1174	27.94	-200
145 C set point 3.52 A, 1800 V	3.51	1800	25.20	-211
100 C set point				

**Table 9. NEXT Thermal Development Test Discharge Data**

Thermal Case	Discharge Current (A)	Discharge Voltage (V)	Cathode Keeper Voltage (V)
Cold Cases:			
Neutralizer Heater (7.2 A, 8.7 V)	0.0	0.0	0.0
Cathode Heater (7.2 A, 13.7 V)	0.0	0.0	-0.2
3.52 A, 1179 V	19.6	24.6	5.5
3.52 A, 1800 V	18.2	23.5	5.4
Ambient Cases:			
Discharge Only (9.1 A, 24.2 V)	9.1	23.2	7.8
4.0 A, 275 V	8.4	25.9	5.4
1.2 A, 679 V	10.0	27.1	4.0
1.2 A, 1179 V	9.2	26.5	4.0
1.2 A, 1800 V	8.9	26.3	3.8
2.0 A, 1179 V	13.9	24.1	4.0
3.52 A, 1179 V	19.6	24.6	5.7
3.52 A, 1800 V	18.2	24.6	6.4
Hot Cases:			
No Thruster Operation	0.0	0.0	0.0
100 C set point			
3.52 A, 1179 V	19.5	24.2	5.5
100 C set point			
3.52 A, 1179 V	19.5	24.1	5.5
145 C set point			
3.52 A, 1800 V	18.3	23.5	5.4
100 C set point			

**Table 10. NEXT Thermal Development Test Neutralizer Data**

Thermal Case	Neutralizer Keeper Current (A)	Neutralizer Keeper Voltage (V)	Coupling Voltage (V)
Cold Cases:			
Neutralizer Heater (7.2 A, 8.7 V)	0.0	-0.4	0.0
Cathode Heater (7.2 A, 13.7 V)	0.0	0.0	0.0
3.52 A, 1179 V	3.0	11.9	-11.6
3.52 A, 1800 V	3.0	11.9	-11.5
Ambient Cases:			
Discharge Only (9.1 A, 24.2 V)	3.0	13.1	0.2
5.0 A, 275 V	3.0	14.3	-10.1
1.2 A, 679 V	3.0	14.2	-10.3
1.2 A, 1179 V	3.0	14.2	-10.4
1.2 A, 1800 V	3.0	14.4	-10.5
2.0 A, 1179 V	3.0	13.4	-11.0
3.52 A, 1179 V	3.0	12.1	-11.4
3.52 A, 1800 V	3.0	12.5	-11.8
Hot Cases:			
No Thruster Operation	0.0	0.0	0.0
100 C set point			
3.52 A, 1179 V	3.0	12.2	-11.4
100 C set point			
3.52 A, 1179 V	3.0	12.2	-11.3
145 C set point			
3.52 A, 1800 V	3.0	12.0	-11.5
100 C set point			

**Table 11. NEXT Thermal Development Test ExB and Tank Temperature Data**

Thermal Case	ExB Shield Plate (C)	ExB Motor Shield (C)	ExB Base Plate (C)	Beam Dump Chevron (C)	Side Wall Back (C)	Side Wall Middle (C)
Cold Cases:						
Neutralizer Heater (7.2 A, 8.7 V)	1	2	2	-4	5	5
Cathode Heater (7.2 A, 13.7 V)	1	3	3	-5	5	5
3.52 A, 1179 V	81	32	32	53	17	10
3.52 A, 1800 V	95	39	40	63	24	18
Ambient Cases:						
Discharge Only (9.1 A, 24.2 V)	1	3	3	-4	5	5
6.0 A, 275 V	4	4	3	-3	6	6
1.2 A, 679 V	27	12	11	11	8	7
1.2 A, 1179 V	28	14	12	14	10	8
1.2 A, 1800 V	36	25	18	21	13	11
2.0 A, 1179 V	51	21	21	30	14	11
3.52 A, 1179 V	82	31	32	52	16	12
3.52 A, 1800 V	97	44	44	67	25	21
Hot Cases:						
No Thruster Operation 100 C set point	3	3	3	-2	7	7
3.52 A, 1179 V 100 C set point	90	48	48	65	26	21
3.52 A, 1179 V 145 C set point	94	53	53	69	29	25
3.52 A, 1800 V 100 C set point	102	53	52	74	31	26

**Table 12. NEXT Thermal Development Test Shroud Temperature Data**

Thermal Case	TC1 (C)	TC2 (C)	TC3 (C)	TC7 (C)	TC8 (C)	TC9 (C)
Cold Cases:						
Neutralizer Heater (7.2 A, 8.7 V)	-175	-183	-184	-180	-176	-178
Cathode Heater (7.2 A, 13.7 V)	-160	-172	-172	-167	-155	-156
3.52 A, 1179 V	-145		-141	-136	-131	-118
3.52 A, 1800 V	-141		-138	-131	-125	-112
Ambient Cases:						
Discharge Only (9.1 A, 24.2 V)	12	16	16	11	10	17
7.0 A, 275 V	13	16	16	10	11	18
1.2 A, 679 V	16	19	19	13	14	22
1.2 A, 1179 V	18	21	21	15	16	23
1.2 A, 1800 V	20	23	23	17	18	26
2.0 A, 1179 V	13	17	18	13	12	21
3.52 A, 1179 V	48	53	52	43	47	57
3.52 A, 1800 V	51	57	56	46	52	61
Hot Cases:						
No Thruster Operation	82	93	102	85	79	89
100 C set point						
3.52 A, 1179 V	84	96	102	86	83	96
100 C set point						
3.52 A, 1179 V	127	141	149	126	127	140
145 C set point						
3.52 A, 1800 V	63	83	105	92	60	77
100 C set point						

**Table 13. NEXT Thermal Development Test Shroud Temperature Data**

Thermal Case	TC10 (C)	TC11 (C)	TC12 (C)	TC13 (C)	TC14 (C)
Cold Cases:					
Neutralizer Heater (7.2 A, 8.7 V)	-185	-183	-127	-183	-189
Cathode Heater (7.2 A, 13.7 V)	-169	-166	-56	-171	-182
3.52 A, 1179 V	-139	-140	-75	-144	
3.52 A, 1800 V	-128	-127	-40	-140	
Ambient Cases:					
Discharge Only (9.1 A, 24.2 V)	16	11	7	17	16
8.0 A, 275 V	16	11	10	17	16
1.2 A, 679 V	19	14	15	20	20
1.2 A, 1179 V	20	16	17	22	21
1.2 A, 1800 V	23	18	20	24	24
2.0 A, 1179 V	17	12	1	19	18
3.52 A, 1179 V	52	45	45	55	55
3.52 A, 1800 V	56	49	52	59	59
Hot Cases:					
No Thruster Operation	96	87	97	95	96
100 C set point					
3.52 A, 1179 V	96	87	70	99	100
100 C set point					
3.52 A, 1179 V	141	128	132	143	145
145 C set point					
3.52 A, 1800 V	95	88	46	88	88
100 C set point					

**Table 14. NEXT Thermal Development Test Heat Flux Coupon Temperature Data**

Thermal Case	Top (C)	Bottom Rear (C)
Cold Cases:		
Neutralizer Heater (7.2 A, 8.7 V)	-56	-136
Cathode Heater (7.2 A, 13.7 V)	-103	-78
3.52 A, 1179 V	-10	-50
3.52 A, 1800 V	-6	-35
Ambient Cases:		
Discharge Only (9.1 A, 24.2 V)	29	17
9.0 A, 275 V	28	19
1.2 A, 679 V	31	23
1.2 A, 1179 V	33	25
1.2 A, 1800 V	35	28
2.0 A, 1179 V	32	18
3.52 A, 1179 V	59	55
3.52 A, 1800 V	63	61
Hot Cases:		
No Thruster Operation	98	103
100 C set point 3.52 A, 1179 V	107	100
100 C set point 3.52 A, 1179 V	147	148
145 C set point 3.52 A, 1800 V	119	96
100 C set point		

**Table 15. NEXT Thermal Development Test Gimbal Flexure Temperature Data**

Thermal Case	GF1	GF1	GF2	GF2	GF3	GF3
	Thruster Side (C)	Gimbal Side (C)	Thruster Side (C)	Gimbal Side (C)	Thruster Side (C)	Gimbal Side (C)
Cold Cases:						
Neutralizer Heater (7.2 A, 8.7 V)	-123	-122	-133	-128	-125	-123
Cathode Heater (7.2 A, 13.7 V)	-31	-41	-31	-41	-31	-42
3.52 A, 1179 V	83	18	85	19	93	25
3.52 A, 1800 V	87	28	95	34	105	39
Ambient Cases:						
Discharge Only (9.1 A, 24.2 V)	58	37	56	33	59	37
10.0A, 275 V	63	42	61	39	64	42
1.2 A, 679 V	75	52	74	48	77	52
1.2 A, 1179 V	76	54	75	50	78	54
1.2 A, 1800 V	78	56	78	53	81	57
2.0 A, 1179 V	87	52	86	49	90	54
3.52 A, 1179 V	124	92	125	89	130	95
3.52 A, 1800 V	129	98	130	96	138	103
Hot Cases:						
No Thruster Operation 100 C set point	95	100	94	97	96	101
3.52 A, 1179 V 100 C set point	154	130	152	123	159	133
3.52 A, 1179 V 145 C set point	184	167	182	163	188	170
3.52 A, 1800 V 100 C set point	154	121	153	114	164	129

**Table 16. NEXT Thermal Development Test Gimbal Pad Temperature Data**

Thermal Case	2 o'clock (L6) (C)	6 o'clock (L6b) (C)	10 o'clock (L6c) (C)
Cold Cases:			
Neutralizer Heater (7.2 A, 8.7 V)	-121	-135	-128
Cathode Heater (7.2 A, 13.7 V)	-25	-25	-26
3.52 A, 1179 V	117	119	129
3.52 A, 1800 V	122	126	144
Ambient Cases:			
Discharge Only (9.1 A, 24.2 V)	72	69	71
11.0A, 275 V	77	74	77
1.2 A, 679 V	91	89	91
1.2 A, 1179 V	91	89	92
1.2 A, 1800 V	93	92	97
2.0 A, 1179 V	108	107	110
3.52 A, 1179 V	146	145	153
3.52 A, 1800 V	152	150	163
Hot Cases:			
No Thruster Operation	94	93	95
100 C set point			
3.52 A, 1179 V	171	171	178
100 C set point			
3.52 A, 1179 V	198	198	204
145 C set point			
3.52 A, 1800 V	176	175	188
100 C set point			

**Table 17. NEXT Thermal Development Test Front Mask Temperature Data**

Thermal Case	Closest to Optics 12 o'clock (L3) (C)	Middle 6 o'clock (L3b) (C)	Closest to Optics 6 o'clock (L4) (C)
Cold Cases:			
Neutralizer Heater (7.2 A, 8.7 V)	-38	-131	-125
Cathode Heater (7.2 A, 13.7 V)	-57	-55	-51
3.52 A, 1179 V	86	68	70
3.52 A, 1800 V	90	73	74
Ambient Cases:			
Discharge Only (9.1 A, 24.2 V)	53	37	39
12.0A, 275 V	56	38	40
1.2 A, 679 V	63	47	48
1.2 A, 1179 V	63	47	48
1.2 A, 1800 V	66	50	52
2.0 A, 1179 V	75	59	60
3.52 A, 1179 V	101	88	88
3.52 A, 1800 V	106	92	92
Hot Cases:			
No Thruster Operation	49	53	52
100 C set point 3.52 A, 1179 V	117	107	106
100 C set point 3.52 A, 1179 V	133	128	124
145 C set point 3.52 A, 1800 V	122	112	110
100 C set point			

**Table 18. NEXT Thermal Development Test Plasma Screen Temperature Data**

Thermal Case	Mask Interface (L5) (C)	Mask Interface (L5b) (C)	Conical Interface (L8) (C)	Conical Interface (L8b) (C)	Rear (L10) (C)
Cold Cases:					
Neutralizer Heater (7.2 A, 8.7 V)	-34	-125	-100	-148	-148
Cathode Heater (7.2 A, 13.7 V)	-51	-56	-41	-47	-5
3.52 A, 1179 V	96	75	78	76	45
3.52 A, 1800 V	100	82	81	91	46
Ambient Cases:					
Discharge Only (9.1 A, 24.2 V)	64	43	57	49	53
13.0A, 275 V	67	43	61	52	55
1.2 A, 679 V	76	52	71	63	62
1.2 A, 1179 V	76	52	71	63	62
1.2 A, 1800 V	78	56	73	68	64
2.0 A, 1179 V	89	66	83	76	68
3.52 A, 1179 V	119	98	120	116	102
3.52 A, 1800 V	124	104	125	124	106
Hot Cases:					
No Thruster Operation 100 C set point	72	66	102	97	98
3.52 A, 1179 V 100 C set point	142	122	151	146	133
3.52 A, 1179 V 145 C set point	165	148	184	179	168
3.52 A, 1800 V 100 C set point	147	129	153	153	127

**Table 19. NEXT Thermal Development Test Ion Optics Temperature Data**

Thermal Case	Stiffening Ring (H10) (C)	Screen Grid Support (H11) (C)	Accelerator Grid Support (H12) (C)
Cold Cases:			
Neutralizer Heater (7.2 A, 8.7 V)	-125	-117	-115
Cathode Heater (7.2 A, 13.7 V)	-11	11	-15
3.52 A, 1179 V	155	210	148
3.52 A, 1800 V	160	209	149
Ambient Cases:			
Discharge Only (9.1 A, 24.2 V)	94	141	97
14.0A, 275 V	95	132	
1.2 A, 679 V	112	150	101
1.2 A, 1179 V	111	143	99
1.2 A, 1800 V	116	145	107
2.0 A, 1179 V	133	172	120
3.52 A, 1179 V	171	221	160
3.52 A, 1800 V	175	222	164
Hot Cases:			
No Thruster Operation	80	76	67
100 C set point			
3.52 A, 1179 V	189	234	175
100 C set point			
3.52 A, 1179 V	209	247	190
145 C set point			
3.52 A, 1800 V	192	232	174
100 C set point			

**Table 20. NEXT Thermal Development Test Harness Temperature Data**

Thermal Case	Downstream (H6) (C)	Cathode Support (H13) (C)	Upstream (H14) (C)	Neutralizer Exit (L9) (C)
Cold Cases:				
Neutralizer Heater (7.2 A, 8.7 V)	-114	-127	-116	-116
Cathode Heater (7.2 A, 13.7 V)	-13	58	-11	-116
3.52 A, 1179 V	154	153	143	-31
3.52 A, 1800 V	164	150	155	80
Ambient Cases:				
Discharge Only (9.1 A, 24.2 V)	88	108	82	79
15.0A, 275 V	91	111	86	57
1.2 A, 679 V	107	124	101	60
1.2 A, 1179 V	107	121	102	70
1.2 A, 1800 V	112	122	107	69
2.0 A, 1179 V	127	140	121	71
3.52 A, 1179 V	171	178	165	83
3.52 A, 1800 V	183	178	178	127
Hot Cases:				
No Thruster Operation	85	93	92	129
100 C set point				
3.52 A, 1179 V	192	197	190	99
100 C set point				
3.52 A, 1179 V	214	220	216	157
145 C set point				
3.52 A, 1800 V	199	193	195	189
100 C set point				

**Table 21. NEXT Thermal Development Test Magnet Temperature Data**

Thermal Case	Front (H1) (C)	Front (H1b) (C)	Cylindrical (H2) (C)	Cylindrical (H2b) (C)	Conical (H3) (C)	Conical (H3b) (C)	Cathode (H4) (C)
Cold Cases:							
Neutralizer Heater (7.2 A, 8.7 V)	-133		-134		-131	-136	-138
Cathode Heater (7.2 A, 13.7 V)	15		5		27	25	130
3.52 A, 1179 V	234		189		201	200	209
3.52 A, 1800 V	232		190		195	193	201
Ambient Cases:							
Discharge Only (9.1 A, 24.2 V)	142	138	106	110	123	121	153
16.0A, 275 V	149	145	113	121	131	128	158
1.2 A, 679 V	171	166	133	143	151	150	172
1.2 A, 1179 V	166	161	134	146	146	142	168
1.2 A, 1800 V	167	162	139	163	147	144	168
2.0 A, 1179 V	200		164		174	169	190
3.52 A, 1179 V	241		203	239	215	213	227
3.52 A, 1800 V	242		209	255	213	214	226
Hot Cases:							
No Thruster Operation	83		89		88	87	89
100 C set point							
3.52 A, 1179 V	258		225		231	229	240
100 C set point							
3.52 A, 1179 V	272		246		251	247	257
145 C set point							
3.52 A, 1800 V	256		221		228	225	234
100 C set point							

**Table 22. NEXT Thermal Development Test Discharge Chamber Temperature Data**

Thermal Case	7 o'clock (H5) (C)	7:30 o'clock (H5b) (C)	8 o'clock (H5c) (C)	8:30 o'clock (H5d) (C)	Propellant Isolator (H7) (C)
Cold Cases:					
Neutralizer Heater (7.2 A, 8.7 V)	-131	-133	-131	-130	-128
Cathode Heater (7.2 A, 13.7 V)	5	6	14	15	-24
3.52 A, 1179 V	189	197	204	196	104
3.52 A, 1800 V	201	210	213	201	105
Ambient Cases:					
Discharge Only (9.1 A, 24.2 V)	104	108	112	119	68
17.0A, 275 V	111	113	117	126	73
1.2 A, 679 V	130	132	137	146	86
1.2 A, 1179 V	133	132	141	143	85
1.2 A, 1800 V	142	140	150	147	87
2.0 A, 1179 V	164	170	175	170	100
3.52 A, 1179 V	197	199	215	210	138
3.52 A, 1800 V	204	203	211	211	142
Hot Cases:					
No Thruster Operation	92	91	90	91	96
100 C set point					
3.52 A, 1179 V	225	231	239	229	165
100 C set point					
3.52 A, 1179 V	249	253	261	249	193
145 C set point					
3.52 A, 1800 V	231	237	239	232	164
100 C set point					

**Table 23. NEXT Thermal Development Cathode Temperature Data**

Thermal Case	NCA Keeper (L1) (C)	NCA Support (L2) (C)	DCA Tube (H8) (C)	DCA Sputter Shield (H9) (C)
Cold Cases:				
Neutralizer Heater (7.2 A, 8.7 V)	485	-41	-133	-138
Cathode Heater (7.2 A, 13.7 V)	-71	-39	469	143
3.52 A, 1179 V	554	107	465	180
3.52 A, 1800 V	551	112	456	181
Ambient Cases:				
Discharge Only (9.1 A, 24.2 V)	487	74	418	144
18.0A, 275 V	551	78	420	147
1.2 A, 679 V	547	89	432	157
1.2 A, 1179 V	548	89	426	155
1.2 A, 1800 V	553	91	424	155
2.0 A, 1179 V	544	102	448	170
3.52 A, 1179 V	558	136	474	200
3.52 A, 1800 V	547	143	469	203
Hot Cases:				
No Thruster Operation	70	102	88	94
100 C set point				
3.52 A, 1179 V	561	165	470	214
100 C set point				
3.52 A, 1179 V	564	194	475	234
145 C set point				
3.52 A, 1800 V	556	172	466	213
100 C set point				

### Acknowledgments

The Thermal Development Test was successfully accomplished through the efforts of a multi-organizational team. The work was performed under the NEXT Project, led by the NASA Glenn Research Center, with Scott Benson as the Project Manager and Mike Patterson as the Principal Investigator. Jon Van Noord, George Soulas, Kevin McCormick, and Daniel Herman of GRC spent a significant amount of time at JPL during the testing described herein and were instrumental in performing this work. Andy Hoskins of Aerojet provided support for the test. At JPL, Allison Owens and Ray Swindlehurst were responsible for designing, configuring, and operating the test facility. Mike Pauken and Phil Stevens helped in the design and measurement of the MLI heat flux coupon boxes. The radiometer for coupon calibration was supplied by JPL's Environmental Test Laboratory and support was provided by Doug Perry. Paul Giuliano, a JPL summer student, helped set up and perform the heat flux coupon calibration. Their efforts and contributions are appreciated.

The research described in this paper was carried out by the Jet Propulsion Laboratory, California Institute of Technology, under a contract with the National Aeronautics and Space Administration.

## References

- <sup>1</sup>M. J. Patterson, J. E. Foster, T. W. Haag, V. K. Rawlin, G. C. Soulas, R. F. Roman, "NEXT: NASA's Evolutionary Xenon Thruster," AIAA 2002-3832, 38<sup>th</sup> AIAA/ASME/SAE/ASEE Joint Propulsion Conference and Exhibit, 7-10 July 2002, Indianapolis, Indiana.
- <sup>2</sup>G. C. Soulas, T. W. Haag, M. J. Patterson, "Performance Evaluation of 40 cm Ion Optics for the NEXT Ion Engine," AIAA 2002-3834, 38<sup>th</sup> AIAA/ASME/SAE/ASEE Joint Propulsion Conference and Exhibit, 7-10 July 2002, Indianapolis, Indiana.
- <sup>3</sup>S. W. Benson, M. J. Patterson, D. A. Vaughan, A. C. Wilson, B. R. Wong, "NASA's Evolutionary Xenon Thruster (NEXT) Phase 2 Development Status," AIAA 2005-4070, 41<sup>st</sup> AIAA/ASME/SAE/ASEE Joint Propulsion Conference and Exhibit, 10-13 July 2005, Tucson, Arizona.
- <sup>4</sup>D. Oh, S. Benson, K. Witzberger, M. Cupples, "Deep Space Applications for NEXT: NASA's Evolutionary Xenon Thruster," AIAA 2004-3806, 40<sup>th</sup> AIAA/ASME/SAE/ASEE Joint Propulsion Conference and Exhibit, 11-14 July 2004, Fort Lauderdale, Florida.
- <sup>5</sup>K. E. Witzberger, D. Manzella, D. Oh, M. Cupples, "NASA's 2004 In-Space Propulsion Refocus Studies for New Frontiers Class Missions," AIAA 2005-4271, 41<sup>th</sup> AIAA/ASME/SAE/ASEE Joint Propulsion Conference and Exhibit, 10-13 July 2005, Tucson, Arizona.
- <sup>6</sup>M. J. Patterson, "NEXT Study of Thruster Extended-Performance (NEXT STEP)," AIAA 2006-4664, 42<sup>nd</sup> AIAA/ASME/SAE/ASEE Joint Propulsion Conference and Exhibit, 9-12 July 2006, Sacramento, California.
- <sup>7</sup>W. A. Hoskins, F. C. Wilson, J. Polaha, L. Talerico, M. J. Patterson, G. C. Soulas, J. Sovey, "Development of a Prototype Model Ion Thruster for the NEXT System," AIAA 2004-4111, 40<sup>th</sup> AIAA/ASME/SAE/ASEE Joint Propulsion Conference and Exhibit, 11-14 July 2004, Fort Lauderdale, Florida.
- <sup>8</sup>Instruction Manual KENDALL RADIOMETER SYSTEM, JPL Publication D-11371, December 1993.
- <sup>9</sup>J. S. Miller, S. H. Pullins, D. J. Levandier, Y. Chiu, R. A. Dressler, "Xenon charge exchange cross sections for electrostatic thruster models," Journal of Applied Physics, V. 91, N. 3, pp. 984-992, 1 February 2002.